Multi-LEO Satellite Networks for Integrated Access and Backhaul

Abubakar Abdulkarim, B. Sc. in Electrical and Electronic Engineering

Submitted in fulfilment of the requirements
for the degree of Master of Science
in Electrical and Computer Engineering

School of Engineering and Digital Sciences
Department of Electrical and Computer Engineering
Nazarbayev University

53 Kabanbay Batyr Avenue,
Nur-Sultan, Kazakhstan, 010000

Supervisors: Prof. Behrouz Maham, Prof. Refik Kizilirmak

15 March, 2024

Declaration

I hereby, affirm that the manuscript titled "Multi-LEO Satellite Networks for Integrated Access and Backhaul" is the outcome of my personal efforts, with the exception of appropriately acknowledged quotations and citations. Furthermore, I attest that to the utmost of my knowledge and conviction, this work has not been previously or simultaneously presented, in its entirety or in part, for the attainment of any other academic certification at either Nazarbayev University or any other national or international academic institution.

. . . .

Signature Date

Abstract

Low Earth Orbit (LEO) Satellites have emerged as a promising solution to extend the coverage area of terrestrial networks, particularly in scenarios where ground users are located in remote or inaccessible areas. As such, forming a network over ground users with LEO satellites becomes essential to ensure reliable connectivity at desired data rates. This thesis focuses on investigating a LEO-network for integrated access and backhaul (IAB) within fifth-generation (5G) systems, where LEO satellites serve as IAB nodes connecting to other IAB nodes for backhaul transmissions while acting as base stations (BSs) for ground users. LEO satellites offer rapid, low-latency connectivity, which is crucial for time-sensitive applications like remote surgery or autonomous vehicles where even slight delays could have significant repercussions. Positioned in a high altitude from the Earth's surface, LEO satellites can achieve remarkably low latency levels, making them comparable to terrestrial networks in terms of responsiveness. Furthermore, the enhanced bandwidth capabilities afforded by LEO satellites position 5G networks optimally to handle the escalating data traffic and increasing number of connected devices effectively. In this work, A model is proposed for wireless multi-hop transmission in LEO satellite networks with integrated access and backhaul (IAB). This model supports ground users that can't communicate directly with ground base stations (gNBs). The traffic flows for uplink and downlink transmissions are characterized using the channel capacity of both local access and backhaul links. LEO-Satellites serve as relay nodes facilitating the link between ground users and gNBs. Additionally, as LEO-Satellites form an interconnected network, they not only communicate with ground users but also engage in data exchange with neighboring LEO-Satellites. Consequently, in the IAB framework, LEO-Satellites transform into IAB nodes, while gNBs act as IAB donors. Within this model, a path is defined by a series of connected LEO-Satellites, and each LEO-Satellite is tasked to deliver data between users and gNBs for uplink and downlink transmissions along the designated path. The proposed model is evaluated by analyzing end-to-end packet transmission delay and propagation delay. Analytical formulas for transmission delay in both the access and backhaul networks are derived, and extensive simulations are conducted to examine the system's sensitivity to various parameters, providing insights into its performance under different scenarios. Furthermore,

analytical expressions for outage probabilities are derived for both the backhaul link, consisting of inter-LEO satellite communication, and access networks connecting LEO satellites with ground users. The channel link in the access network is assumed to follow a Nakagami fading channel, while the backhaul network is primarily influenced by large-scale fading. Through numerical simulations, the impact of transmission rate and LEO-Sat transmit power on the system's outage probability is analyzed, revealing trade-offs between data rate and reliability. To efficiently allocate transmit power to LEOs and support the specified data rates of ground users, an optimization problem is formulated and solved to minimize the total transmit power of LEOs.

Acknowledgement

Praise be to Allah (S.W.A), I express my deep gratitude to my special mentor Senior Professor Behrooz Maham for unwavering support and encouragement in my academic endeavors. Professor Maham not only provided valuable knowledge on the topic but also encouraged me to explore new areas related to my research topic. His prompt response and patient response, even in difficult situations, played a vital role in overcoming obstacles and greatly relieved my stress I owe the success of my research to his guidance , which I really appreciate. Moreover, I would like to thank my co-supervisor, Assistant Professor Refik Kizilirmak, for his time and ongoing support. I am also grateful to the Department of Electrical and Computer Engineering and the administrative staff of Nazarbayev University for giving me the opportunity to pursue a master's degree. Their collective efforts contributed to a rich educational experience. Finally, my heartfelt gratitude goes to my family and friends for their unwavering support and encouragement throughout my study journey.

Table of Contents **Page No.**

Chapter 1- Introduction

1.1 Background

The surge in global mobile data traffic due to increased end-user population and demand for data-intensive services has prompted the need for network densification. This involves deploying more ground new base station (gNB) to enhance coverage and capacity. However, with each new BSs node added, the requirement arises to efficiently route data to the Core Network (CN). Conventionally, this data backhauling process is executed through the resource-intensive and costly installation of optical fiber cables. As such this network densification faces challenges, notably the high cost of deploying optical fiber connections for gNBs [1]. This cost arises from trenching and installation operations. To address this, the utilization of wireless channels, commonly referred to as wireless backhauling is proposed as an alternative. In 3GPP releases 16 and 17 [2,3], 3GPP proposed integrated access and backhaul (IAB) for replacing the fixed fiber backhauling between gNB with wireless backhauling. It is also known as self-backhauling, since the backhaul, links can be controlled as wireless access links by the gNB itself. It becomes more beneficial in the mmWave spectrum since the coverage is limited and, therefore, the number of gNBs or small cells increases. Within densely interconnected networks, where conventional fiber cable backhauling might prove impractical or costly, IAB offers an efficient, viable alternative. This can be largely attributed to the substantial bandwidth inherent in the mmWave spectrum [4–6]. As outlined by the 3GPP specifications, the architecture of an Integrated Access and Backhaul (IAB) network comprises two essential components: an IAB donor and IAB nodes [7]. An IAB node serves as an access network node, facilitating access links to User Equipments (UEs) as well as backhaul links connecting to either other IAB nodes or the designated IAB donor. On the other hand, the IAB donor is a gNB that operates as a pivotal network element, extending network access to UEs through a network of access and backhaul links [8].

Exploiting the advantages offered by its substantial bandwidth and small wavelength, mmWave (IAB) facilitates the implementation of extensive beamforming. This approach effectively allocates a portion of the cost-effective bandwidth to accommodate the backhaul process. Given that high band spectrum is often structured as unpaired, the operational framework of

IAB proposed by 3GPP enables both wireless in-band and out-of-band relaying strategies [9].

- In-band relaying: This approach involves the simultaneous transmission of both access and backhaul links within the same frequency band.
- Out-of-band relaying: In this scenario, the transmission of access and backhaul links takes place in distinct and orthogonal channels. Precisely, the access link operates within a designated frequency band, while the backhaul link utilizes the remaining available frequency band.

The future wireless network vision is centered on ensuring universal connectivity for all, anytime and anywhere. This covers even the most remote rural areas and scenarios like ships, airplanes, and oceans, where traditional terrestrial network nodes are impractical. Using non-terrestrial networks (NTNs), such as geostationary earth orbit (GEO), medium Earth orbit (MEO) satellites, and low earth orbit (LEO) satellites for IAB operations emerges as a promising solution. This approach not only bridges connectivity gaps in underserved regions but also eases terrestrial network congestion during peak demands. Furthermore, the rising number of satellites in Earth's orbit emphasizes the significance of IAB operations in efficiently utilizing spectrum within the evolving domain of non-terrestrial networks.Satellite-terrestrial communication offers a notable benefit by allowing network operators to achieve expansive coverage with reduced expenses.

Currently, various projects, including SpaceX and OneWeb, are actively pursuing satellite-terrestrial communication initiatives. These endeavors are focused on establishing global coverage and delivering high data rates through LEO-Sat networks. In this context, the design of the backhaul link connecting satellites and terrestrial infrastructure significantly influences user service quality [9].

1. 2 Aims and objectives

This research work aims to investigate IAB using Non-Terresterial Networks (NTN) and develop a robust wireless multi-hop transmission model named Multi-LEO-Sat networks for IAB. This model will cater to the requirements of IAB, enabling ground users without direct communication links to gNBs to establish connectivity through multi-hop transmissions. The traffic

patterns for uplink and downlink transmissions is characterized using the channel capacity of local access and backhaul links.There exist several metrics, including but not limited to latency, reliability, energy consumption, capacity, and scalability, which can be utilized to evaluate the performance of a given system.

In this research, we use several channel models to examine how IAB via Multi-LEO satellites might be enhanced in terms of reliability and latency. We believe that employing the reliability metric in the context of outage probability is advantageous because it aids in evaluating the error performance and robustness of communication links over long distances, ensuring successful data transmission between LEO satellites and ground infrastructure.It also provides information on the IAB system's end-to-end connectivity. Furthermore, it affords valuable insights into the end-to-end connectivity of the IAB system. This involves assessing the reliability of both the access links (connecting ground users and LEO-Sats) and the backhaul links (connecting LEO-Sats and ground new base stations), consequently ensuring a thorough evaluation of the entire network. On the other hand, latency assumes a pivotal role in evaluating the efficiency of backhaul connectivity between LEO-Sats and ground new base stations. Low latency guarantees the swift and reliable transmission of data, thereby contributing to the overall performance of the integrated system. Furthermore, this work expolored the impact of various parameters on the system's performance.

Moreover, we formulate an optimization problem aimed at reducing the overall transmit power of LEO-Sats along a specified path, considering the data rates required for uplink and downlink transmissions of ground users along that path. Upon obtaining the solution to this optimization problem, it is utilized for allocating power to the LEO-Sats.

1. 3 Methodologies and techniques

We design a Multi-LEO-Sat network IAB with the purpose of providing support to ground users who are unable to establish direct connections with gNBs. LEO-Sats serve as intermediary nodes that facilitate the connectivity between ground users and gNBs. However, due to the fact that LEO-Sats are interconnected to form a network, each LEO-Sat can not only communicate with ground users, but also to exchange data with neighboring LEO-Sats. Consequently, in

accordance with the concept of IAB, LEO-Sats assume the role of IAB nodes, while gNBs act as IAB donors. In order to transmit data from one LEO-Sat to another via wireless backhaul and facilitate the downlink and uplink transmissions of ground users at each LEO-Sat, a multi-hop transmission model is considered. Based on the multi-hop transmission model, a path can be characterized by a set of connected LEO-Sats, where each LEO-Sat is to deliver data between users and gNBs for uplink and downlink transmissions through the path (it is also assumed that each end node of a path is a gNB). We assume two different types of wireless systems for the multi- LEO-Sat network. One is to exchange data packets between LEO-Sats, which is referred to as LEO-Sat network for backhauling. As per the IAB standard, this LEO-Sat-network serves as the backhaul network. The second category involves a local access network for each LEO-Sat, saving a particular footprint, in order to facilitate communication between LEO-Sat and the ground users located within it is footprint. We also discuss the throughput analysis for a given path in a multi- LEO-Sat network, where we derive channel link capacity of LEO-Sat-Network. For the first part of the work we assume a scenario, where there exist no multi-path components over the interlinks among the LEO-Sats and the links between satellites and ground users in each access network.As such only large scale fading and pathloss are consider. Thus, we analyse the system base on packet transmission delay. In the second scenario, we assume that the channel link in the access network follows nagakami channel model. Therefore, we analyse the performance of the system using both reliability (outage probability) and latency (delay outage).

For the literature review using trustworthy digital libraries such as Elsevier, IEEE XploreDigital Library, Scopus, and others. For performance evaluation sections, we use Wolfram Mathematica software, and for simulations, we use MATLAB software.

1.4 Thesis structure

This research project is organized as follows: The 2nd chapter presents a thorough assessment of the literature on the strategies presented by scholars in this field. This chapter also includes an overview of the most prevalent metrics for performance evaluation. Chapter 3 is dedicated to Multi-LEO-Sats for IAB where both the access and backhaul network, are assumed to only

affected by large scale fading and pathloss. This chapter includes system model, the throughput of a path that consists of multiple LEO-Sats, where each LEO-Sat becomes a flying BS for uplink and downlink transmissions of associated ground users. Additionally performance evaluation, and numerical results subsections are all presented. Chapter 4 is dedicated to combining large scale fading channels and Nakagami-m fading channels, where the access network link assumed to follow nakagami fading channel, and the link between LEO-Sats are assumed to be affected by only large scale fading. These chapter also include system model, performance evaluation, and numerical results subsections. We investigate the throughput of a route comprising several LEO-Sats, where each LEO-Sat serves as a flying base station for both uplink and downlink transmissions of linked ground users. Additionally, we formulate an optimization problem aimed at minimizing the total transmit power of LEO-Sats in Section 5. In Chapter 6, the findings are succinctly summarized, research gaps and limitations are identified, and directions for future investigation are determined.

Chapter 2 – Literature review

2. 1 Introduction

The exponential growth in both end-user population, such as smartphone and tablet users, and the demand for information services, including video streaming and cloud computing, has led to a significant surge in global mobile data traffic in recent years [10]. Predictions indicate that by 2030, the volume of global mobile traffic is anticipated to escalate by 670 times compared to 2010 [11]. To accommodate this exponential growth in traffic, there is an expectation for a significant increase in the density of base stations (BSs) in the foreseeable future. The concept of denser BS deployments, often referred to as network densification, has been explored as a potential solution to cope with the escalating traffic demands [12]. Network densification aims to extend the coverage area and meet the high capacity demands by reducing the distance between mobile users and BSs, thereby enhancing spectrum reuse [13].

However, a major drawback of conventional network densification lies in the substantial capital and operational costs associated with optical fiber deployment for BSs. In urban areas, for instance, the estimated cost of deploying one meter of optical fiber ranges from 100-200 USD, with approximately 85% of the total expenditure attributed to trenching and installation operations [14]. In light of these challenges, wireless backhaul presents an attractive implementation solution compared to conventional wired-optical-fiber backhaul. Wireless backhaul offers comparable transmission rates to optical fiber, while also providing significant cost reductions and greater flexibility and timeliness in deployment, with no intrusive installation processes [15]. Furthermore, a key objective of 6G communications is to achieve worldwide connectivity [16]. This necessitates providing reliable communication services in remote and rural areas, where the use of wireless backhaul may be economically appealing compared to wired-optical-fiber backhaul. In Long-Term Evolution (LTE) Rel-10, the 3GPP introduced the concept of wireless backhaul, known as LTE relaying [17]. However, due to the high value of spectrum resources in LTE, there was limited commercial interest in backhauling. With the rollout of several nationwide 5G mobile networks and the allocation of 5G licenses for commercial use, there is a significant emphasis on leveraging high-frequency transmitting carriers, such as mmWave, to accommodate larger spectrum requirements [18]. However, the use of

high-frequency carriers is constrained by limited coverage area, necessitating higher density deployments of BSs. The development of 5G NR by 3GPP aims to address the requirements for higher system capacity, improved coverage, and increased data rates [19]. Ultra-lean transmission, cutting-edge antenna technologies, and spectrum flexibility, particularly the ability to operate in high-frequency bands, are important architectural tenets of 5G NR. [20]. Utilizing the wide bandwidth available in 5G NR, operators can partition the entire radio resource into two component for wireless backhauling and access, respectively. This approach, known as IAB networks, has garnered significant research attention [21, 22]. Standardized as a cost-effective alternative to wired backhauling by 3GPP, IAB NR networks are increasingly gaining industrial interest [23]. Particularly in mmWave networks, the demand for wireless backhauling is heightened due to coverage limitations, while the use of larger bandwidths reduces costs for operators, and the employment of numerous antennas enhances signal directional gain and link reliability for backhauling.

2. 2 Non-Terrestrial IAB Networks

The aspiration to achieve global connectivity has long been recognized [24]. In pursuit of this goal, satellite and unmanned aerial vehicle (UAV) technologies have emerged as appealing options for providing communication services in areas that are economically prohibitive or logistically challenging for conventional terrestrial networks to reach, such as rural and remote regions, as well as marine areas [25]. This section explored research pertaining to non-terrestrial IAB networks, categorizing these studies into two main groups: (i) UAV for IAB networks and (ii) satellite-terrestrial IAB networks.

2.2.1 UAV for IAB Networks

The mobility and relocation flexibility of Unmanned Aerial Vehicle Base Stations (UAV-BSs) enable their deployment at any desired three-dimensional (3D) position. However, in a realistic environment, the presence of non-negligible multipath propagation and link blockage poses a significant challenge in optimizing the positions of UAV-BSs within UAV-assisted networks. In [26], the authors utilized ray-tracing simulations to investigate the coverage gains of UAV-assisted millimeter-wave (mmWave) IAB networks, where UAV-BSs serve as IAB nodes. By

considering amplify-and-forward (AF) OBFD and decode-and-forward (DF) IBFD modes, optimal UAV positions were determined through ray tracing-based coverage maps. Simulation results demonstrated a 31% improvement in downlink (DL) coverage gains with the AF mode outperforming the DF mode. [27] explores the feasibility of utilizing low altitude platform aircraft, specifically UAVs, to facilitate connectivity for remote devices. This is examined with two distinct types of UAVs: static UAVs and mobile UAVs. In [28], the focus is on positioning devices and collecting data using a mobile UAV in conjunction with multiple Base Stations (BSs). Similarly, [29] looks into data collection via a mobile UAV, presenting optimization challenges to maximize device coverage while adhering to constraints like storage and latency. Despite these contributions, the existing studies, such as [27, 28], largely revolve around the usage of a single UAV. In contrast, our work centers on employing multiple LEOs within an IAB network to serve remote ground users. Notably, our study accounts for both uplink and downlink transmissions for ground users, a dimension not fully explored in [27, 29].

Past studies have also investigated multi-UAV scenarios. For instance, [30] employs static UAVs to bolster downlink transmissions for ground users, assigning one UAV per user. The coordination of trajectory and communication for multiple mobile UAVs is explored in [31]. Nevertheless, these studies assume no direct communication links between UAVs, indicating that each UAV may either have a direct link to a ground Base Station (gNB) or possess stored data and UAVs do not form a network by themselves for IAB. In our approach, we establish a network by interconnecting multiple LEO satellites for IAB purposes.In an IBFD UAV-assisted IAB network, the combined optimization problem of the number and 3D placements of UAV-BSs was addressed in [32]. In order to maximize the total transmission rate while decreasing the number of UAVs, they presented a heuristic algorithm. The suggested approach reduced the data rate block ratio and enhanced overall throughput, according to numerical results.The UAV-BS placement problem was addressed by [33] in order to optimize the sum rate and the number of mobile users served. Investigations into the effects of mobile users' movements revealed strong performance under user mobility. In order to address the joint optimization problem of UAV-BS position and bandwidth allocation, [34] defined a piecewise-linear function of acquired transmission rate. They proposed a heuristic algorithm to maximize the total net-

work profit, outperforming established solvers such as BARON and the NEOS platform. [35] developed analytical frameworks to characterize the performance of a UAV-assisted mmWave IAB network with terrestrial BSs (TBSs) and UAV-BSs, considering dynamic changes in multipath propagation and link blockage. Results showed that increasing the intensity of UAV-BS traversals improved outage probability (OP) and spectrum efficiency, and lower flight speeds enhanced wireless backhaul performance.

Importantly, in IAB scenarios, LEOs not only facilitate data exchange for backhaul transmissions but also function as Base Stations for ground users' uplink and downlink communications. As a result, our research presents a comprehensive model encompassing the intricacies of wireless multi-hop transmissions within LEO-networks.

2.2.2 Satellite-terrestrial IAB networks

Satellite communication networks utilize spaceborne platforms which includes Low Earth Orbit (LEO) satellites, Medium Earth Orbit (MEO) satellites, and Geosynchronous Earth Orbit (GEO) satellites. In recent years, there has been a notable resurgence in interest towards broadband provision facilitated by LEO satellite networks (SatNets), characterized by extensive satellite constellations such as Starlink, Kuiper, OneWeb, and Lightspeed. With their capability to establish inter-satellite networks, LEO SatNets are poised to play a pivotal role in future integrated networks. This innovative satellite architecture holds the promise of revolutionizing traditional communication networks, offering benefits including service continuity, wide-area coverage, and support for critical communications and emerging applications like Internet of Things (IoT) devices/Machine-to-Machine (M2M) communication and intelligent transportation systems, while enabling network scalability.

The investigation of the integration between satellite and terrestrial networks has been examined in [36, 37]. In [36], a beamforming strategy for cognitive satellite-terrestrial networks was suggested, leveraging a combination of a base station and a cooperative terminal to bolster secrecy performance. Additionally, [38] addressed the challenge of optimizing the sum rate in networks that integrate satellites and airborne terrestrial components. This involved tackling the problem of multicast communications with rate-splitting multiple access. In [39], the au-

thors presented a novel concept involving a hybrid geostationary orbit (GEO) satellite terrestrial backhaul network. They successfully addressed the challenge of optimizing spectral efficiency in backhaul links through a solution to the carrier allocation problem. Meanwhile, the authors in [40] proposed a terrestrial-satellite architecture that seamlessly integrates ultra-dense LEO networks with terrestrial systems to facilitate efficient data offloading. Their primary goal, centered around maximizing the sum data rate, revealed a notable performance advantage of integrated satellite-terrestrial networks over their non-integrated counterparts. Additionally, the study detailed in [41] concentrated on an integrated LEO-satellite and terrestrial network for offloading purposes. Specifically, the focus was on incentivizing data offloading between a satellite operator and a terrestrial operator for satellite-backhauled network access. The outcomes demonstrated the existence of an optimal LEO satellite density to strike a balance between the utility and cost of data offloading for both operators. The authors in [42],presents a case study examining the viability of integrating LEO satellites into an in-band IAB operation. The study explores both orthogonal and non-orthogonal bandwidth allocation between access and backhauling, considering both time- and frequency-division duplex (TDD/FDD) transmission modes. Numerical findings from the study demonstrate the viability of IAB via satellites and highlight the superior performance of FDD transmission compared to TDD.

Furthermore, the problem of assigning spectrum resources for downlink (DL) transmission in a satellite-terrestrial integrated access and backhaul (IAB) network was addressed by [43]. The assumption behind this system is that the same frequency bands are available to satellite and terrestrial communications. The Hungarian technique was utilized to successively discover the optimal strategy for carrier allocation by breaking down the challenge of maximizing the overall data rate into two smaller issues. An architectural framework for a satellite-terrestrial IAB network with a data offloading focus was examined in [44]. Terrestrial links use the C-band frequency, whereas links linking satellite and terrestrial nodes for backhaul use the Ka-band bandwidth. Mobile users on ground can utilize macro-cells, small-cells, or or LEO-based small-cells to connect to the core network. To optimize the total data rate, a modified swap matching algorithm was proposed to establish optimal policies for user connectivity, subchannel assignment, and power management. Simulation outcomes suggested that the overall network capacity is

not solely reliant on the projected satellite area, implying the existence of an optimal satellite deployment strategy to maximize the aggregate backhaul capacity.

In [45] a pricing mechanism for data offloading based on the Stackelberg game model applied to a satellite-terrestrial IAB network. To address the growiing demand for backhaul at conventional Access Points (APs), they proposed shifting some user demand from conventional APs to LEO-based APs. In this setup, LEO-based APs assume the role of leaders while conventional APs act as followers. An iterative algorithm was suggested to reach the Stackelberg equilibrium, where the optimization problem at the follower level aimed at optimizing user connectivity using fractional programming, followed by the optimization problem at the leader level focusing on setting service prices and allocating the Ka-band spectrum using alternative optimization techniques. Simulation results illustrated an optimal density of LEO satellites to balance the trade-off between AP utility and cost. In [46], the authors focused on delay performance in mega LEO constellations. The study explored the use of ground-based relays to establish low-latency wide-area networking for LEO constellations. For forthcoming mega-constellations like Starlink, the authors discussed two intercontinental connections, suggesting that implementing ISLs could mitigate latency and enhance capacity during network congestion.

In [47], researchers analyzed time delay and outage performance across various transmission scenarios in LEO mega-constellations. They proposed analytical models to assess end-to-end time delay and outage performance under different transmission conditions. The authors presented numerical results to validate these models and compare performance metrics, concluding that the size of the coverage area of LEO satellites had a minor negative impact on time delay. In [48], the authors works on the reliability of downlink transmission in LEO satellite communication systems. They derived a novel expression for the outage probability of LEO satellite transmission and simulated LEO satellite communication scenarios considering severe Doppler effects. System performance was evaluated using the Orthogonal Time Frequency Space (OTFS) scheme and traditional Orthogonal Frequency Division Multiplexing (OFDM) scheme through simulations.

Chapter 3 – Multi-LEO Satellite Networks for Integrated Access and Backhaul Under Large Scale Fading

Due to the higher altitude of LEO-Sats, for this scheme we assume that the channels between the ground user and LEO-Sat can establish line-of-sight (LoS) communication, with the propagation primarily influenced by distance and large-scale fading effects [49]

3. 1 System Model

Consider a ommunication system with multiple LEO-Sats and two gNBs, i.e., a source gNBs and a destination gNBs. Each LEO-Sat is assigned a specific area called a footprint, denoted by Q_m for the m^{th} LEO-Sat. The ground users within the footprint Q_m communicate with LEO-Sat m. The entire area of interest is divided into M footprint, i.e., Q_m, $m = 1, \ldots, M.$, one for each LEO-Sat. For example, in Fig.1, we consider $M = 4$. The source gNBs is responsible for sending data packets to the ground users, which is known as the downlink transmission. Conversely, the destination gNBs may receives data packets from the ground users, representing the uplink transmission. It is important to note that in practical scenarios, the role of a gNBs as a source or destination may not be fixed. Unlike a conventional cellular system where a Base Station (BS) handles both downlink and uplink transmissions, in this case, a gNBs can assume either the source or destination role as needed. This flexibility allows for a more generalized communication setup. In addition to the forward path (source gNBs to ground users and destination gNBs), there is also a reverse path where the roles of the source and destination gNBs are reversed. This means that the source gNBs can become the destination gNBs, and vice versa. This flexibility enables bidirectional communication and accommodates different traffic flows. In the multi-LEO-Sat network, we consider two wireless systems with distinct purposes. The first system, known as the LEO-Sats-network, facilitates the exchange of data packets between LEO-Sats and serves as the backhaul network. This network follows IAB standard and enables efficient communication between the LEO-Sats. The second system is the local access network, which is dedicated to each footprint in the network. For instance, Q_m represents a specific footprint associated with LEO-Sat m. The local access network supports direct communication between

LEO-Sat m and the ground users located within the coverage area of that particular footprint. In this manner, multiple local access networks are established in the multi-LEO-Sats network to facilitate communication between LEO-Sats and ground users within their respective coverage areas.

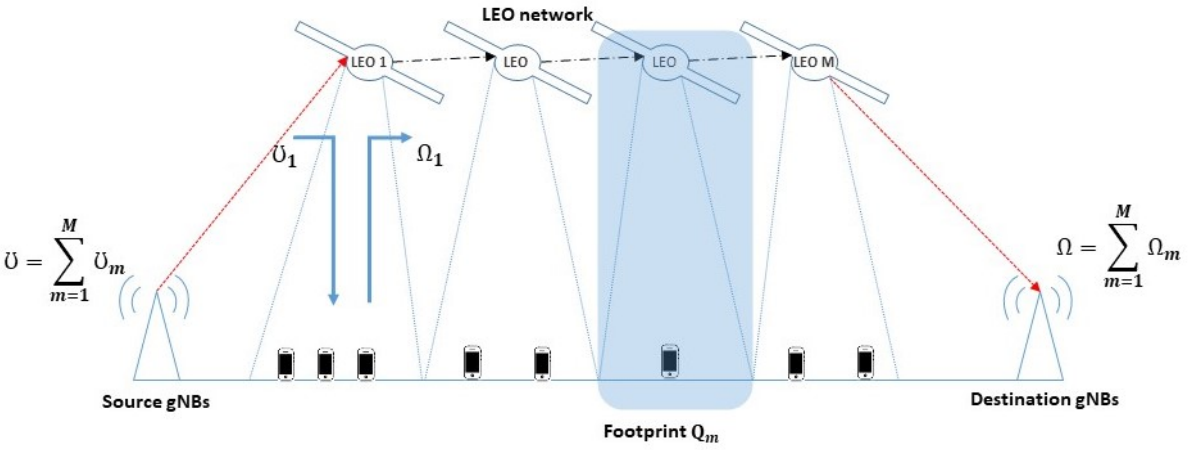

Fig. 1. A multi-LEO-Sats Network with a source and destination gNBs.

3.2 Throughput Analysis of a Path

In this section, we discussed the analysis of the throughput for a specified path within a multi-LEO-Sat network. It is assumes that the traffic within the network is represented by data flows, with the average values for downlink and uplink denoted as $\mho_m$ and Ω_m in Q_m, respectively.

3. 2. 1 LEO-Sats Network Link Capacity

We examine the LEO-Sat network, where LEO-Sats utilize full-duplex transceivers. Consequently, LEO-Sat m can transmit its signal to LEO-Sat $m+1$ while simultaneously receiving signals from LEO-Sat $m-1$. The communication link connecting LEO-Sat m and $m+1$ is known as LEO-Sat link, with LEO-Sat m as the transmitter and LEO-Sat $m+1$ as the receiver within the LEO-Sat network. Considering the higher altitude of LEO-Sats, we can assume that they establish LoS communication, with the propagation primarily influenced by distance and large-scale fading effects. Assuming that LEO-Sats have perfect antenna alignment and that the communication path between LEO-Sats can be approximated as a straight line. Therefore LEO-Sats experience no interference from the signals transmitted by the preceding and succeeding

LEO-Sat. Thus, the capacity of LEO-Sat link $m, m = 0, 1, \cdots, M$, is given by

$$c_m = \log_2 \left(1 + \frac{P_{\text{Leo},m} d_{m,m+1}^{-\alpha} G_{m,m+1}}{\sigma^2} \right), \tag{1}$$

where $P_{\text{Leo},m}$ represents the transmission power of LEO-Sat m for LEO-Sat link, whereas $G_{m,m+1}$ represents the antenna gain of LEO-Sat m in the direction of LEO-Sat $m+1$, $d_{m,m+1}$ is the distance between LEO-Sat m and LEO-Sat $m+1$, and α represents the path loss exponent, σ^2 is the noise power at the receiver of LEO-Sat network.

3. 2. 2 Downlink and Uplink of Local Access Networks

It is assumed that each LEO-Sat has the capability to establish a downward beam, providing support to users within its coverage area, as depicted in Fig.1. In terms of user association, we consider that the users in coverage area Q_m are exclusively linked with LEO-Sat m. Consequently, this means that no (inter-)interference stemming from other coverage areas is considered in when determining the downlink and uplink capacity for each specific coverage area.

Let N_m represent the total number of ground users within coverage area Q_m. Assuming symmetrical conditions as discussed in [50], where the channels from the LEO-Sat to the associated ground users possess identical statistical properties, The uplink channel linking the ground user to LEO-Sat m and downlink channel connecting LEO-Sat to ground user both follow free space pathloss model having a channel gain denoted by $g_{m,k}^u$ and $g_{m,k}^d$ respectively. The received SNR over the link between LEO-Sat m and ground user in the footprint Q_k in the downlink and the received SNR at the LEO-Sat m in the uplink is given by

$$\mu_m^d = \frac{P_{\text{Loc},m} g_{m,k}^d}{\sigma^2}, \tag{2}$$

and

$$\mu_m^u = \frac{P_g \sum_{n=1}^{N_m} g_{m,k}^u}{\sigma^2}, \tag{3}$$

where $g_{m,k}^i = \dfrac{G_{ue} G_{\text{Leo}} b(\phi_{m,k}^i)}{l_{m,k}^i}, i \in \{u, d\}$ and $l_{m,k}^i = \dfrac{16\pi^2 {f_c}^2 {D_{m,k}^i}^\alpha}{c^2}$ denote the free space path loss;

$D_{m,k}$ represent the distance between the LEO-Sat m and the ground user within coverage area Q_k as shown in Fig.2 G_{Leo} and G_{ue} in the channel gain expression are the maximum antenna gains of the LEO-Sat and ground user respectively; $\phi_{m,k}$ the bore-sight angle from LEO-Sat m to user in footprint Q_k. Moreover, P_g is the transmit power of ground users, $P_{\text{Loc},m}$is the transmit power of LEO-Sat in Q_k, and $b(\phi)$ in the channel gain formula denote the LEO-Sat beam gain pattern function which varies based on the ground user location and is express as

$$b(\phi) = \begin{cases} 1 & ,\phi = 0, \\ 4\left|\frac{J_1(ka\sin\phi)}{ka\sin\phi}\right| & ,\phi \neq 0, \end{cases} \tag{4}$$

where $k = 2\pi f_c/c$, c, a, and f_c are the speed of light, antenna aperture radius, and frequency, respectively.

The distances $D^u_{m,k}$ and $D^d_{m,k}$ can be express respectively as

$$D^u_{m,k} = \sqrt{{r_e}^2\ \sin^2\zeta_m + h^2 + 2r_e h}\ -\ r_e\ \sin\zeta_m, \tag{5}$$

where ζ_m represent the elevation angle between the ground source horizon plane and the LEO-Sat m.

$$D^d_{m,k} = \sqrt{{r_e}^2\ \sin^2\varphi_m + h^2 + 2r_e h}\ -\ r_e\ \sin\varphi_m, \tag{6}$$

where r_e represent the radius of the Earth, h denote the altitude of the LEO-Sat, and φ_m represent the elevation angle between the ground user's horizon plane and the LEO-Sat m.

3. 3 Delay Performance Analysis

In this work, ground-based users transmit data packets to their intended destinations through the backhaul link of LEO-Sat, all within the mmWave frequency bands. Our study specifically takes into account the influence of LOS components in the mmWave spectrum, with our analysis focusing on the considerations of large-scale fading and path loss effects.

To assess how well the proposed system performs with respect to transmission delay, the total end-to-end communication time should be determined. This overall communication delay

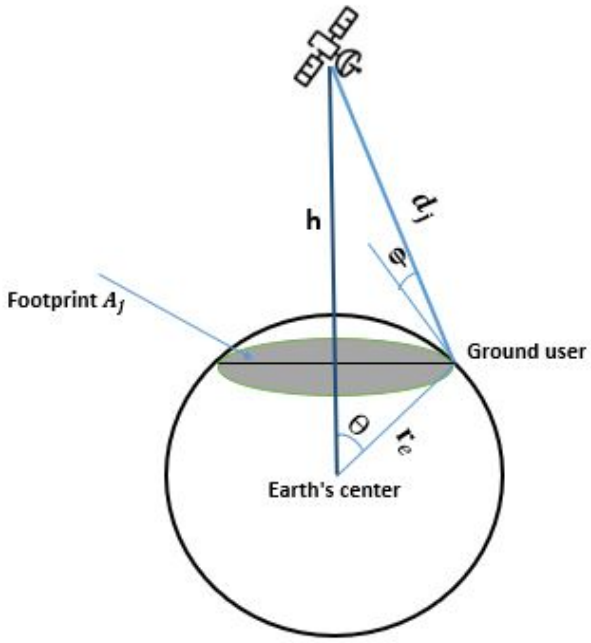

Fig. 2. Footprint zone of LEO-Sat.

includes both the time required for transmission and the time needed for signal propagation, which collectively facilitate the transfer of data packets from the ground source to the ground destination via the LEO-Sat network. Propagation time accounts for the time taken for the signals to travel through the local access networks and LEO-Sat network. While transmission time encompasses the time required for encoding, framing, and transmitting the data packets through the local access networks and LEO-Sat network.

3. 3. 1 Delay Analysis in the Access Networks

For the access network, we take into account uplink and downlink transmissions and propagation times. The total time of packets delivery for uplinks in the access network can be express as

$$T_u = T_{pr,u} + T_{tr,u}, \tag{7}$$

where $T_{tr,u}$ is packets transmission time from the ground user to the LEO-Sat m, $T_{pr,u}$ is propagation time from the ground user to LEO-Sat m.

It is important to note that in satellite technologies, the time it takes for signals to propagate

is longer compared to terrestrial communication systems [51]. As a result, these propagation delays must be considered when assessing the system's performance. The uplink propagation time can be expressed as [52]

$$T_{pr,u} = \frac{D^u_{m,k}}{c}, \tag{8}$$

where $D^u_{m,k}$is given in the expression in (5), and c is the speed of light.

The transmission time of packets for uplinks in the access network can be obtained from expression in (3) using the Shannon formula as

$$T_{tr,u} = \frac{S}{B_a \log_2\left(1 + \frac{P_g \sum_{n=1}^{N_m} g^u_{m,k}}{\sigma^2}\right)}, \tag{9}$$

where S represents the packet size, B_a denotes the access channel bandwidth.

Similarly, for the downlink the total time of packets delivery in the access network can be express as

$$T_d = T_{pr,d} + T_{tr,d}, \tag{10}$$

where $T_{tr,d}$ is packets transmission time from the LEO-Sat m satellite to the ground user, $T_{pr,d}$ is propagation time from LEO-Sat m to the ground user.

$T_{pr,d}$ and $T_{tr,d}$ can be expressed from the expression in (2), and using Shannon formula as

$$T_{pr,d} = \frac{D^d_{m,k}}{c}, \tag{11}$$

and

$$T_{tr,d} = \frac{S}{B_a \log_2\left(1 + \frac{P_{\text{Loc},m} g^d_{m,k}}{\sigma^2}\right)}, \tag{12}$$

respectively, where $D^d_{m,k}$is given in the expression in (6).

3. 3. 2 Delay Analysis in the LEO-Sat Networks

We consider the cross-section of the earth as a circular shape as in Fig.3, the distance between two consecutive LEO-Sat m and $m+1$, can be represented by the length of a chord, which is given by

$$d_{m,m+1} = 2(h+r_e)\sin\frac{\theta}{2}, \tag{13}$$

where h is the height of LEO-Sat from the ground, r_e is the radius of the earth and θ the angle subtends by the chord. Therefore the overall distance between LEO-Sat 1 to a LEO-Sat M can be expressed as

$$\begin{aligned} D_{\text{Leo}} &= \sum_{m\in\{1\leq m<M\}} d_{m,m+1} \\ &= 2(M-1)(h+r_e)\sin\frac{\theta}{2}, \end{aligned} \tag{14}$$

Thus, the propagation time of the packets in (LEO-Sat network can be expressed as

$$T_{pr,\text{Leo}} = \frac{D_{\text{Leo}}}{c}, \tag{15}$$

Moreover, using the expression in (1), the packets transmission time in the backhaul link can be expressed using the Shannon formula as

$$T_{tr,\text{Leo}} = \frac{S}{B_b \log_2\left(1+\frac{P_{\text{Leo},m} d_{m,m+1}^{-\alpha} G_{m,m+1}}{\sigma^2}\right)}, \tag{16}$$

Consequently, the total transmission time of packets in the LEO-Sat network can be obtained from (15) and (16) as

$$\begin{aligned} T_{\text{Leo}} &= T_{pr,\text{Leo}} + T_{tr,\text{Leo}} \\ &= \frac{D_{\text{Leo}}}{c} + \frac{S}{B_b \log_2\left(1+\frac{P_{\text{Leo},m} d_{m,m+1}^{-\alpha} G_{m,m+1}}{\sigma^2}\right)}, \end{aligned} \tag{17}$$

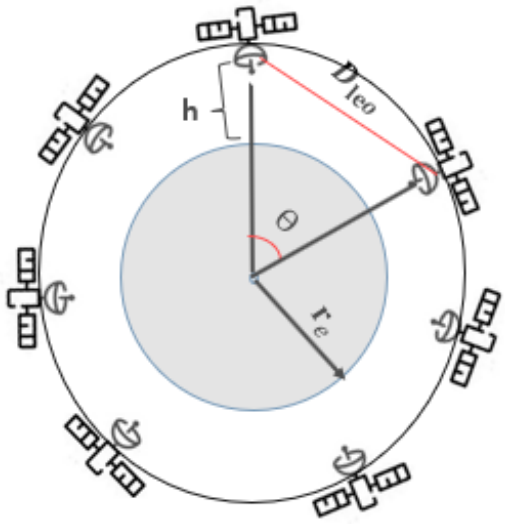

Fig. 3. Transmission between LEO-Sat.

Then, it is easy to obtain the end-to-end time for packets to be transmitted from the ground source to the ground destination through the LEO-Sat network by combining equations (7), (10), and (17) as

$$\begin{aligned} T_{\text{e2e}} &= T_u + T_{\text{Leo}} + T_d \\ &= T_{pr,u} + T_{tr,u} + T_{pr,\text{Leo}} + T_{tr,\text{Leo}} + T_{pr,d} + T_{tr,d} \\ &= \frac{D^u_{m,k}}{c} + \frac{S}{B_a \log_2\left(1 + \frac{P_g \sum_{n=1}^{N_m} g^u_{m,k}}{\sigma^2}\right)} + \frac{D_{\text{Leo}}}{c} \\ &+ \frac{S}{B_b \log_2\left(1 + \frac{P_{\text{Leo},m} d^{-\alpha}_{m,m+1} G_{m,m+1}}{\sigma^2}\right)} + \frac{D^d_{m,k}}{c} \\ &+ \frac{S}{B_a \log_2\left(1 + \frac{P_{\text{Loc},m} g^d_{m,k}}{\sigma^2}\right)}, \end{aligned} \tag{18}$$

3. 4 Numerical Result

In this section, we provide numerical findings for the evaluation of transmission delays within the proposed Multi-LEO-Sat integrated access and backhaul system. These evaluations are conducted using a variety of system parameters. Therefore, we carry out experiments using a free-

space path-loss model that solely considers the impact of transmission distance. In pursuit of this objective, we illustrate the transmission delay within the backhaul of the LEO-Sat network, as well as the combined transmission delay of the access network and backhaul network. We analyze alterations in transmission delay by varying the number of LEO-Sats and adjusting the elevation angle of these satellites. Table I provides a summary of the various parameters utilized in our numerical analysis.

Table 1. System Parameters

Parameter	**Value**
Total transmit power P	0 dBm - 50 dBm
Noise PSD σ^2	-174 dBm/Hz
UE antenna gain	0 dBi
LEO-Sat altitude	600 Km
Packets size S	50 Mbits
Speed of light c	3×10^8 m/s
Earth radius r_e	6371 Km
Total channel bandwidth	400 MHz
Number of ground user N_m	20
LEO-Sat antenna gain $G_{\text{Leo}}$and G_{ue}	63 dB
Path-loss exponent α	2
Frequency f_c	28×10^9 Hz

3. 4. 1 Delay Analysis in the Backhaul Network

The numerical analysis employs a free-space path-loss channel model. Fig.4, illustrates the impact of transmit power on backhaul performance. In this regard, we consider a range of transmit power P varies from 0 to 50 dBm, with all LEO-Sats transmitting at the same power level. Notably, the observed pattern indicates that higher transmit power values lead to decreased transmission delay in the backhaul, as depicted by the curves.

From Fig.5, we can observe the relationship between backhaul network performance and different channel bandwidth values in the context of a free-space path-loss channel model. Within this analysis, we explore the impact of different backhaul channel bandwidths B_b ranging from 100 to 500 MHz, while varying the number of LEO-Sats $M = 2$, 3, 5, 7, and 10. The trend is apparent: as the channel bandwidth increases, the transmission delay curves for the system show a consistent decrease.

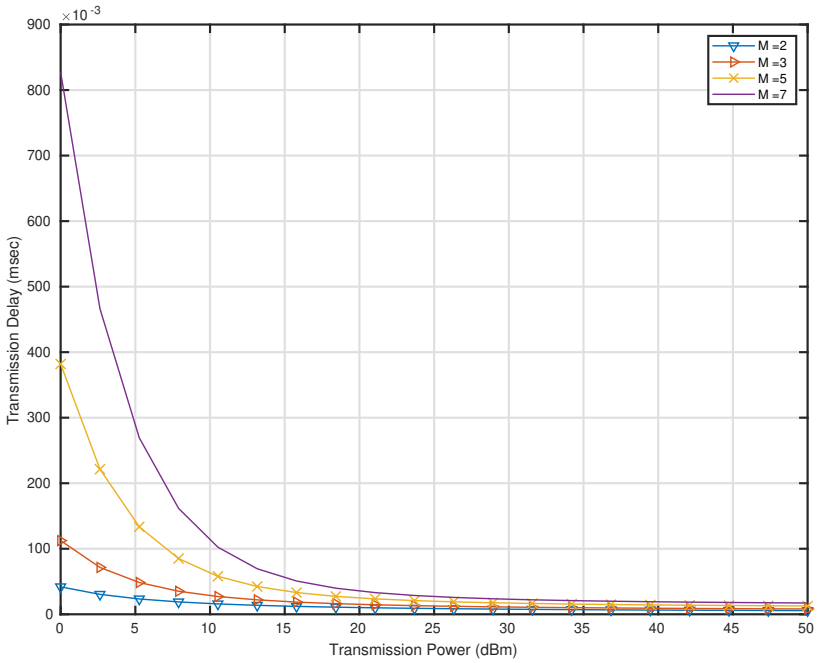

Fig. 4. The transmission delay curves of backhaul network with B_b = 300 MHz, S = 50 Mbits, h = 600 km versus transmit power for different number of LEO-Sats.

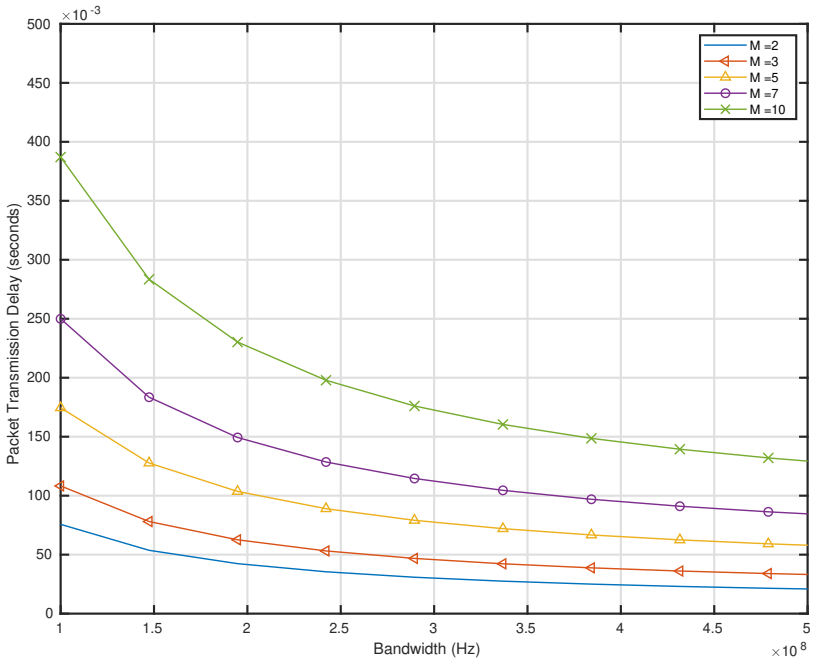

Fig. 5. The transmission delay curves of LEO-Sat network with P = 30 dBm, S = 50 Mbits, h = 600 km versus channel bandwidth for different number of LEO-Sats.

3. 4. 2 End To End Delay Analysis

In this subsection, we investigate the end-to-end transmission delay i.e., considering the uplink backhaul link and downlink altogether. In Fig. 6, shows the system latency performance dependency on transmit power. Thus, we assume transmit power, i.e., P varies from 0 to 50 dBm, the elevation angle is φ = 10, 15 degrees, and the number of LEO-Sats is M = 2, 5. From the analysis, we can see that the transmission delay curves of the system decrease with higher values of transmit power. In addition, the system latency performance improves with higher value of LEO-Sat elevation angle. Fig.7, displays how the end-to-end system's transmission

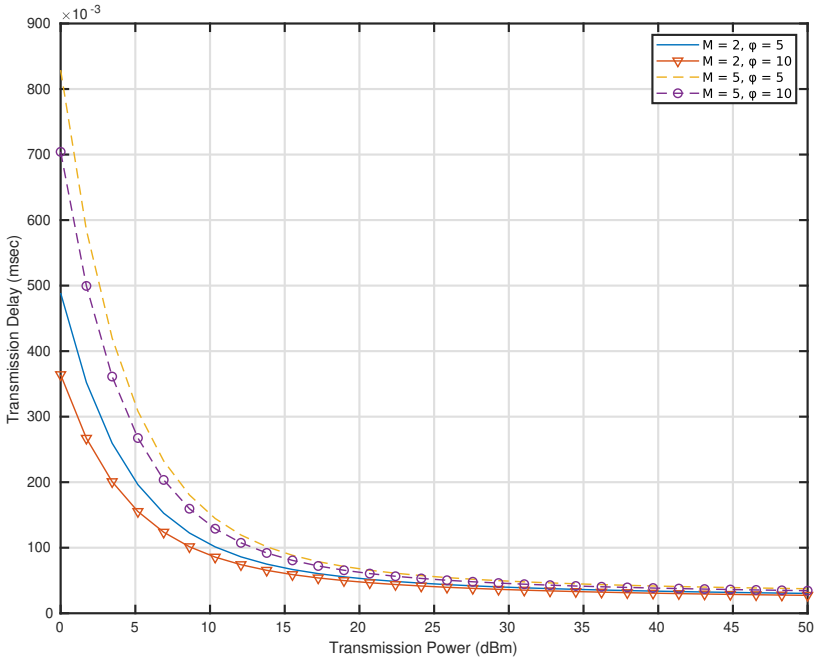

Fig. 6. The end-to-end transmission delay curves with B_b = 300 MHz, B_a = 100 MHz, S = 50 Mbits, h = 600 km versus transmit power for different elevation angle values and different number of LEO-Sats.

delay performance is influenced by packet size under free-space path-loss channel model. Notably, as the packet size S increases from 50 to 400 Mbits, there is a corresponding rise in the transmission delay curves. Similarly, higher value of LEO-Sat elevation angle, i.e., φ = 10, 15 degrees, leads to the decrease of the transmission delay curves of the system.

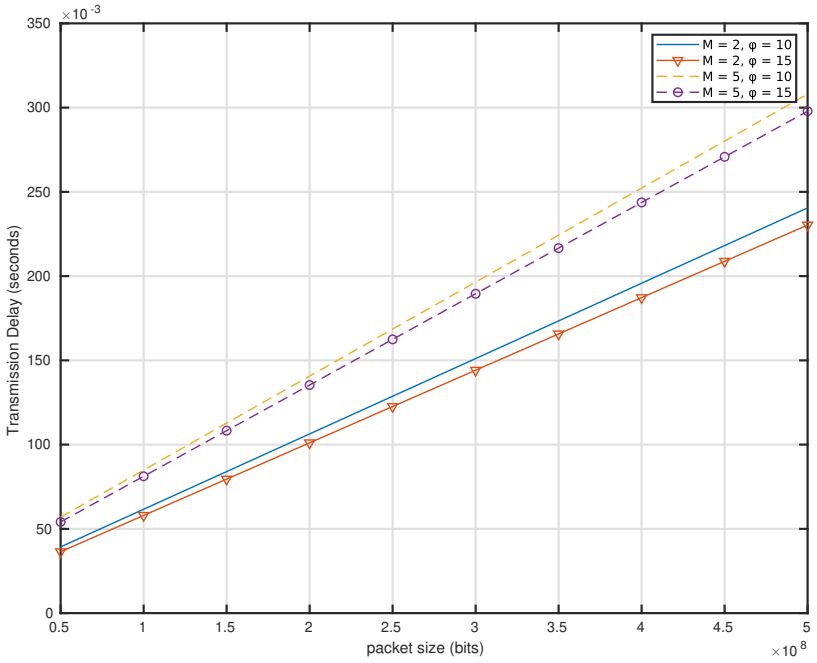

Fig. 7. The end-to-end transmission delay curves with P = 30 dBm, B_b = 300 MHz, B_a = 100 MHz, h = 600 km versus packet size for different number of LEO-Sats and different elevation angle values.

Chapter 4 – Multi-LEO Satellite Networks for Integrated Access and Backhaul Under Nakagami Fading Channel

In this section we investigate the outage probability analysis of a IAB-based LEO-Sat network. In this network, we consider the Nakagami-m model for both access and bachaul links, which allows us to incorporate the impact of both LOS and NLOS conditions. LEO-Sats serve as relay nodes connecting ground users with gNBs. Within the notion of IAB framework, LEO-Sats becomes IAB nodes, while gNBs act as IAB donors. The network operates on a multi-hop transmission model, where interconnected LEO-Sats form paths for data exchange, supporting both uplink and downlink transmissions for ground users.

4.1 System Model

In this section, we consider a multi-LEO-Sat network comprising multiple LEO-Sats, termed as IAB nodes, ground users, and ground base stations, referred to as IAB donors. Following 5G standards, a ground base station is denoted as a gNB for convenience. Unlike traditional cellular systems, we explore a scenario where ground users are unable to establish direct communication with gNBs. Instead, they communicate with associated LEO-Sats, given their location outside the coverage of any gNB due to the sparse deployment of gNBs.

4.1.1 A Multi-LEO-Sats Network

We assume there are J LEO-Sats. Each LEO-Sat is dedicated to a specific area known as a footprint, denoted by A_j for the j^{th} LEO-Sat, and ground users within A_j establish communication with LEO-Sat j. The area of interest is subdivided into J footprints, namely A_j, where $A_j, j = 1, \cdots, J$. To illustrate, consider a scenario with $J = 3$, as depicted in Fig.1. Alongside LEO-Sats, there exist two gNBs: a source and a sink gNB. From a ground user's perspective, the source gNB is responsible for transmitting data packets to the user (downlink), while the sink gNB receives data packets from the user (uplink). However, in practice, a gNB may not be confined to a fixed role as a source or sink gNB, unlike a conventional cellular system where a BS communicates with users for both downlink and uplink transmissions. Therefore, for generalization, we can contemplate an additional path, the reverse path, where the source gNB switches roles with the sink gNB and vice versa. For simplicity, we focus on one path, as illus-

trated in Fig.8. Furthermore, we consider two distinct wireless systems within the multi-LEO-Sat network. The first involves the exchange of data packets among LEO-Sats, identified as the LEO-network for backhauling, as per the IAB standard designating it as the backhaul network. The second system constitutes an access network for each footprint, denoted as A_j, facilitating communication between LEO-Sat j and the ground users within this footprint. Therefore, the multi-LEO-Sat network comprises one LEO-network and J access networks.

4.1.2 LEO-Sat Network as a Backhaul Network

For a LEO-Sat network, we can examine a route as depicted in Fig.8. We represent the average bit rates transmitted to and received from the ground users in footprint A_j by Υ_j and β_j, respectively. Additionally, we denote Υ and β to indicate the average aggregation rates received from the source gNB to LEO-Sat 1 and from LEO-Sat J to the sink gNB, respectively, i.e.,

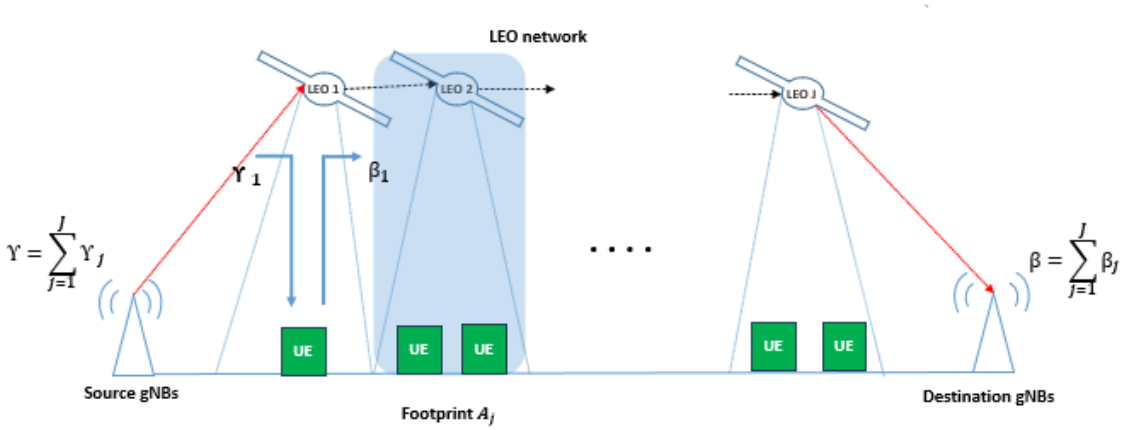

Fig. 8. A multi-LEO-Sats Network with access and backhaul links.

$$\Upsilon = \sum_{j=1}^{J} \Upsilon_j \quad \text{and} \quad \beta = \sum_{j=1}^{J} \beta_j, \tag{19}$$

Subsequently, the average bit rates sent from LEO-Sat j to LEO-Sat $j+1$ through the backhaul link becomes

$$\Omega_j = \Upsilon + \sum_{n=1}^{j} \beta_n - \sum_{n=1}^{j} \Upsilon_n = \sum_{n=j+1}^{J} \Upsilon_n + \sum_{n=1}^{j} \beta_n, \tag{20}$$

where $\Omega_0 = \Upsilon$ and $\Omega_J = \beta$.

4.1.3 Access Networks

As previously stated, there exist J access networks, each containing one LEO-Sat and corresponding ground users. To simplify, within each access network, a downlink signifies a connection from the LEO-Sat to a ground user, whereas an uplink represents a connection from a ground user to the LEO-Sat. Consequently, in access network j, the overall transmission rates for downlink and uplink are denoted as Υ_j and β_j, respectively.

4.2 Transmission in the LEO-Sat Network

In this section, we consider the LEO-Sat network, wherein LEO-Sats employ full-duplex transceivers as documented in [53]. Consequently, LEO-Sat j has the capability to transmit its signal to LEO-Sat $j+1$, simultaneously receiving signals from LEO-Sat $j-1$. The channel between LEO-Sats j and $j+1$ is referred to as LEO-Sat-link j, where LEO-Sats j and $j+1$ function as the transmitter and receiver, respectively, in the LEO-Sat network. Given the elevated altitude of LEO-Sats, we can assume a clear line-of-sight (LoS) condition, with propagation being predominantly influenced by distance or large-scale fading. Therefore, the capacity of LEO-Sat-link j, $j = 0, 1, \cdots, J$, is given by

$$C_j = \log_2 \left(1 + \frac{P_{Leo,j} d_{j,j+1}^{-\alpha} |h_{j,j+1}|^2 G_j G_{j+1}}{q \sigma^2} \right), \tag{21}$$

where $P_{Leo,j}$ is the transmission power of LEO-Sat j for LEO-Sat link, whereas G_j and G_{j+1} represents the antenna gain of LEO-Sat j and LEO-Sat j respectively, $d_{j,j+1}$ is the distance between LEO-Sat j and LEO-Sat $j+1$, and α represents the path loss exponent. In addition, $h_{j,j+1}$ is the normalized channel gain to model the small-scale fading. Moreover, σ^2 is the noise power at the receiver of LEO-Sat network and q is the free-space unit-distance transmission pathloss expressed as $q = \left(\frac{4\pi}{\lambda}\right)^2$, where λ is the wavelength value.

4.2.1 Outage Performance in the Backhaul Link

The outage probability (OP) refers to the likelihood that the received signal-to-noise ratio (SNR) falls below a specified threshold. In the context of the link between LEO-satellite j and LEO-satellite k the OP can be expressed as

$$P_{\text{out}}^{j,k} = \Pr\left\{\mu_{j,k} \leq \mu_{th}\right\}, \tag{22}$$

where $\mu_{th} = 2^{R/W} - 1$ is the specified threshold, and R and W are achievable data rate and bandwidth, respectively.

As mentioned in previous chapter we consider the cross-section of the earth as a circular shape as in Fig.3, the distance between two consecutive LEO-Sat j and $j+1$, is given by (13) Therefore, the overall distance between LEO-Sat 1 to a LEO-Sat J can be expressed as

$$D_{\text{Leo}} = \sum_{j\in\{1\leq\ j<J\}} d_{j,j+1}, \tag{23}$$

Hence, the OP for LEO-network communications from LEO-satellite 1 to LEO-satellite J can be determined by

$$P_{\text{out}}^{\text{Leo-net}} = 1 - \prod_{j\in\{1\leq\ j<J\}} \left(1 - P_{\text{out}}^{j,j+1}\right), \tag{24}$$

where

$$P_{\text{out}}^{j,j+1} = \Pr\left\{\frac{P_{Leo,j} d_{j,j+1}^{-\alpha} |h_{j,j+1}|^2}{G_j^{-1} G_{j+1}^{-1} q\, \sigma^2} \leq \mu_{th}\right\}, \tag{25}$$

Note that in the simulation results, it is assumed that all LEO satellites employ a uniform transmit power, denoted as P_{Leo}, and that inter-neighboring LEO satellite communications have an identical transmission distance. The end-to-end outage probability for the LEO-network, i.e., backhaul link, experiences the minimum impact from the small-scale fading characteristics of the wireless channel, and thus, the backhaul channels can be considered deterministic. This

observation can be attributed to the following two factors: First, the transmission distance between adjacent LEO satellites is predetermined and very slowly change once the number of satellites per orbital plane is established during the signaling phase of the satellite system. Secondly, the key characteristic of RF signal propagation in outer space is the absence of multipath propagation. Unlike traditional terrestrial wireless communication systems, where signals can experience multiple paths due to reflection, diffraction, and scattering, inter-LEO satellite transmissions in outer space exhibit a clear and direct signal propagation path without the presence of multipath components. However, our formulation is general and in case backhaul channels are modelled as Nakakami-m, $|h_{j,j+1}|^2$ in (25) is Gamma distributed and $P_{\text{out}}^{j,j+1}$ is simply cumulative distribution function (CDF) of a Gamma distributed random variable.

4.3 Downlink and Uplink Transmission in Access Networks

It is supposed that each LEO-Sat possesses the capability to establish a downward beam to cater to the users within its coverage area, as depicted in Fig.8. Regarding user association, we posit that users within coverage area A_j are exclusively associated with LEO-Sat j. Consequently, in the determination of downlink and uplink capacity for each coverage area, we do not account for any interference originating from other footprints.

4.3.1 Outage performance in the uplink and downlink of the access network

Similar to [54], we consider the Nakagami-m model for access links, which allows us to incorporate the impact of both LOS and non-line-of-sight (NLOS) conditions. Furthermore, we assume that the parameter m, which represents the Nakagami channel model, takes integer values. Mathematically, the relationship between m and the powers associated with LOS and NLOS is given by $K = \frac{\sqrt{m^2-m}}{m-\sqrt{m^2-m}}$ [55]. The parameter K represents the ratio of LOS power to NLOS power. By observing the relationship, it becomes evident that with an increase in the value of m, the influence of the LOS component becomes increasingly prominent. If the value of m is large, $K \approx 2m$ which is specifically applicable in situations where there is a significant presence of the LOS component. It is important to highlight that due to unavoidable obstacles and shadowing, there is no deterministic communication channel between the LEO satellite and the ground use.

We assume the utilization of analog beamforming for both transmitters and receivers to address the pathloss effect caused by long range communications or by the high frequency bands employed in millimeter wave communications. The uplink channel coefficient linking the ground user to LEO satellite j and downlink channel coefficient connecting LEO satellite to ground user are both Nakagami-m distributed denoted by g_j^u and g_j^d, respectively. The received SNR over the link between LEO satellite j and ground user in the footprint A_j in the downlink and the received SNR at the LEO satellite in the uplink is given by

$$\mu_j^d = \frac{P_{Leo,j} G_{Loc,j} G_{Leo,j} |g_j^d|^2}{\sigma^2}, \tag{26}$$

and

$$\mu_j^u = \frac{P_{ue} \sum_{n=1}^{N_j} G_{Loc,n} G_{Leo,n} |g_n^u|^2}{\sigma^2}, \tag{27}$$

with their average values $\bar{\mu}_j^d = \frac{P_{Leo,j} G_{Loc,j} G_{Leo,j} \Omega_j^d}{\sigma^2}$ and $\bar{\mu}_j^u = \frac{P_{ue} \sum_{n=1}^{N_j} G_{Loc,j} G_{Leo,j} \Omega_j^u}{\sigma^2}$, respectively, where $P_{Leo,j}$ is the transmit power of LEO-Sat j in the access network, P_{ue} is the transmit power of ground users, $G_{Leo,j}$ and $G_{Loc,j}$ are the maximum antenna gain at j^{th} LEO-Sat adjusted toward the footprint A_j and maximum antenna gain of the ground user in the access network, respectively. Furthermore, the average power gain of access channels, Ω_j^i, which is influenced by the inverse of the path-loss, can be computed as follows:

$$\Omega_j^i = E\left\{ \left| g_j^i \right|^2 \right\} = \frac{c^2}{16\pi^2 {f_c}^2 {d_j^i}^{\alpha}}, \text{ where i} \in \{u, d\} \tag{28}$$

where c is the speed of light, α is the path-loss exponent, f_c denotes carrier frequency, and d_j^i the distance between the ground user and LEO-satellite j as shown in Fig.3. The distances d_j^u and d_j^d are equivalently express respectively in (5) and (6).

Given our assumption that the uplink and downlink channels follow independent Nakagami-m models, we can describe μ_j^d and μ_j^u as a random variables following a Gamma distribution with a parameters $\bar{\mu}_j^d$ and $\bar{\mu}_j^u$, respectively, with a Nakagami channel parameter m_i. Assuming

an integer values form_i, the distributions of μ_j^d and μ_j^u takes on the Erlang form, and its CDF can be expressed as

$$F_{\mu_j^d}(x;m_i) = 1 - e^{-\frac{x}{\bar{\mu}_j^d} m_i} \sum_{k=0}^{m_i-1} \frac{1}{k!} \left(\frac{x}{\bar{\mu}_j^d} m_i \right)^k, \text{ for } x \geq 0, \tag{29}$$

and

$$F_{\mu_j^u}(x;m_i) = 1 - e^{-\frac{x}{\bar{\mu}_j^u} m_i} \sum_{k=0}^{m_i-1} \frac{1}{k!} \left(\frac{x}{\bar{\mu}_j^u} m_i \right)^k, \text{ for } x \geq 0 \tag{30}$$

respectively. The occurrence of an outage occurs when either μ_j^u, μ_j^d, or both, decline below a specific threshold, μ_{th}. Hence, the outage probability, for both the uplink and downlink can be computed as

$$P_{\text{out}}^{u,d} = \Pr\left\{ \mu_j^u \leq \mu_{th} \,||\, \mu_j^d \leq \mu_{th} \right\}. \tag{31}$$

The expression in (31) can be further simplified as

$$P_{\text{out}}^{u,d} = \Pr\left\{ \min(\mu_j^u, \mu_j^d) \leq \mu_{th} \right\}. \tag{32}$$

The expression in (32) can be written as

$$\begin{aligned} P_{\text{out}}^{u,d} &= 1 - \Pr\left\{ \mu_j^u > \mu_{th} \right\} \Pr\left\{ \mu_j^d > \mu_{th} \right\} \\ &= 1 - (1 - P_{\text{out}}^u) \left(1 - P_{\text{out}}^d \right). \end{aligned} \tag{33}$$

Therefore, the end-to-end outage probability can be expressed as

$$P_{\text{out}}^{\text{e2e}} = 1 - (1 - P_{\text{out}}^u) \left(1 - P_{\text{out}}^d \right) \times \prod_{j \in \{1 \leq j < J\}} \left(1 - P_{\text{out}}^{j,j+1} \right). \tag{34}$$

Since in the backhaul link, LOS component is dominant due to the lack of barriers and free space environment, i.e $m \to \infty$, we assume the channel is deterministic. With an appropriate value of μ_{th}, it is nearly error-free; thereby resulting in no outage at backhaul links, i.e.,

$P_{\text{out}}^{j,j+1} = 1$. However, as it is mentioned in Section 4.2.1, in case backhaul links are modelled as Nakagami-m channels, $P_{\text{out}}^{j,j+1}$ is CDF of Gamma or Erlang similar to the expression in (29).

Using (29), we have

$$P_{\text{out}}^{u} = \Pr\left\{\mu_j^u \leq \mu_{th}\right\} = 1 - F_{\mu_j^u}(\mu_{th}; m_i). \tag{35}$$

Accordingly, using (30), we can also obtain

$$P_{\text{out}}^{d} = 1 - F_{\mu_j^d}(\mu_{th}; m_i). \tag{36}$$

Therefore, we have

$$\begin{aligned} P_{\text{out}}^{\text{e2e}} &= 1 - \left(F_{\mu_j^u}(\mu_{th}; m_i)\right)\left(F_{\mu_j^d}(\mu_{th}; m_i)\right) \\ &= 1 - e^{-\frac{\mu_{th}}{\bar{\mu}_j^u} m_i} \sum_{k=0}^{m_i-1} \frac{1}{k!}\left(\frac{\mu_{th}}{\bar{\mu}_j^u} m_i\right)^k \\ &\quad \times e^{-\frac{\mu_{th}}{\bar{\mu}_j^d} m_i} \sum_{k=0}^{m_i-1} \frac{1}{k!}\left(\frac{\mu_{th}}{\bar{\mu}_j^d} m_i\right)^k. \end{aligned} \tag{37}$$

4.4 Numerical Results

This section presents numerical results to showcase the performance of the analytical findings discussed in the preceding section within the proposed multi-LEO-Sat integrated access and backhaul system. Similar to [56], we consider a carrier frequency of 30 GHz, a path-loss exponent of 2, and a Nakagami parameter is set to $m = 2$. All RF chains are assumed to have a maximum antenna gain of 30 dB. Moreover, adhering to the typical channel bandwidth for 5G systems we assume a channel bandwidth of $W = 300$ MHz. We additionally consider a LEO-Sat altitude of 600 km, a noise spectral density of $\sigma^2 = -174$ dBm/Hz, an Earth radius of r_e = 6378 km, and the speed of light as $c = 3 \times 10^8$ m/s. The parameters utilized in the system simulation are summarized in Table 2.

Fig.9 depicts the outage probability for the ground user in relation to the transmission rate R

Table 2. System Parameters

Parameter	Value
LEO transmit power P_{Leo}	15, 30, and 30 dBm
Noise PSD σ^2	-174 dBm/Hz
LEO-Satellite altitude h	600 km
Speed of light c	3×10^8 m/s
Earth radius r_e	6371 Km
Total channel bandwidth	300 MHz
Maximum antenna gain G_{Leo} and G_{Loc}	60 dB
Path-loss exponent α	2
Nakagamai parameter m	2
Frequency f_c	30×10^9 Hz

across three distinct transmitting power levels of the LEO-Sat in the access network, denoted as P_{leo}. As R increases, there is a concurrent escalation in the outage probability, consistent with its defined behavior. Furthermore, the simulations indicate a decrement in the outage probability curves of the system with increased values of the transmit power of LEO-Sat.

Fig.10 illustrates the impact of the average transmit power of the ground user on system efficiency, when the achievable data rate of $R = 7$ Mbps is considered. The transmit power P_{ue} is varied from 0 to 30 dBm, while the elevation angle φ is set to 5, 20, 40, and 60 degrees. As anticipated, higher values of transmit power result in improved system performance. Furthermore, the simulation demonstrates enhanced system performance associated with higher elevation angle values of LEO-Sats.

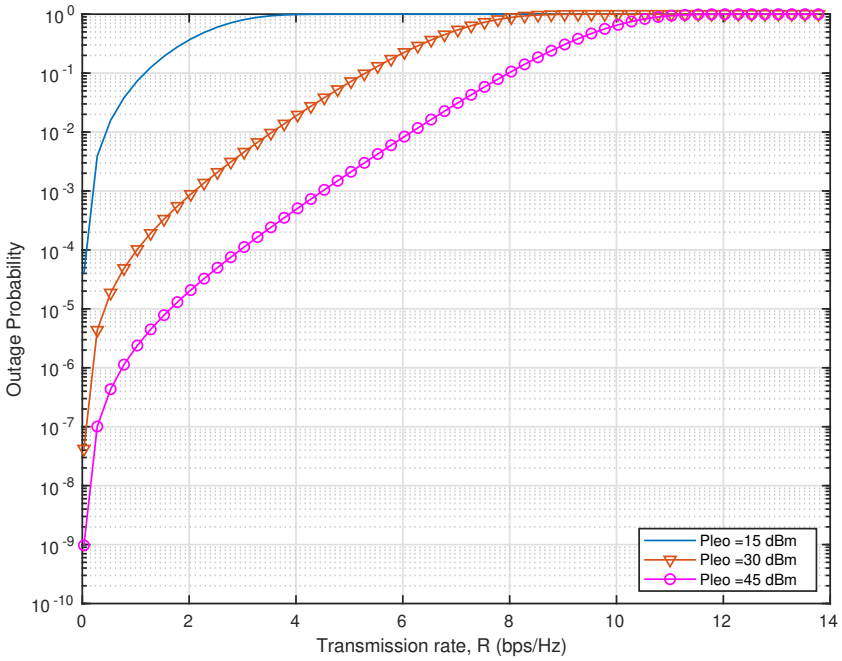

Fig. 9. The system performance evaluated as outage probability curves versus the transmission rate R for different transmitting power levels of the LEO-Sat in the access network P_{leo}.

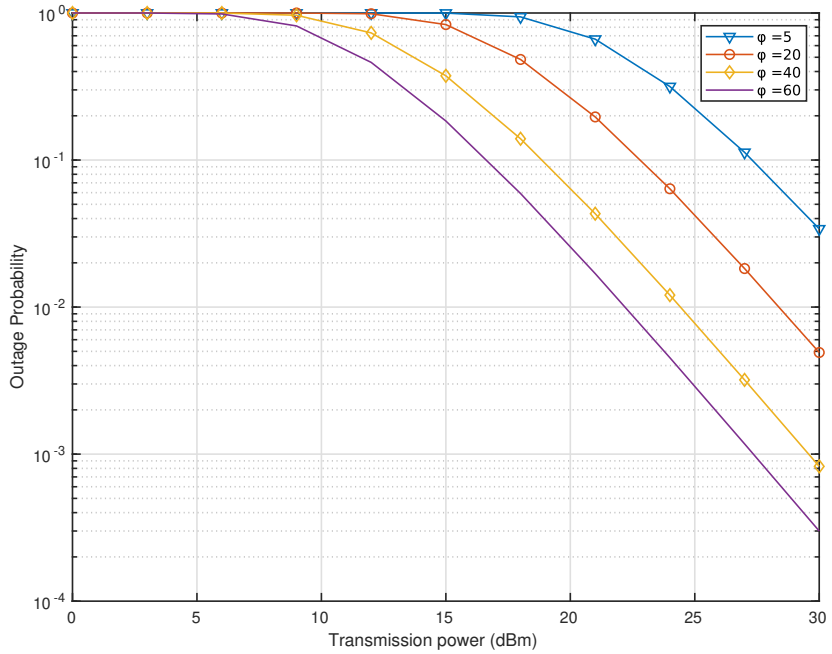

Fig. 10. The end-to-end outage probability curves for a system model with a bandwidth of W= 300 MHz and a satellite altitude of h= 600 km versus average transmit power of the ground user P_{ue} for different elevation angle values.

Chapter 5 – Throughput Analysis and Total Transmit Power Minimization Problem of LEO-Sat Network

In this section, we analyze the throughput of a route comprising multiple LEO-Sats, each serving as an aerial BS facilitating uplink and downlink transmissions of associated ground users, An optimization problem is then formulated to reduce the overall transmit power of the LEO-Sats.

5.1 Throughput Analysis of A Muilti-LEO-Sat Network

In the previous section, we denote the average bit rates transmitted to and received from ground users within footprint A_j as Υ_j and β_j, respectively. Furthermore, Υ and β given by (19) represent the average aggregation rates received from the source gNB to LEO-Sat 1 and from LEO-Sat J to the sink gNB, respectively.

5.1.1 LEO-Sat-Network Link Capacity

As LEO-Sats operate at very high altitudes, it is reasonable to assume that they sustain LoS links, with propagation predominantly affected by distance or large-scale fading. Hence, the capacity of uplink channel is given by (1). However, (1) does not account for the interference due to LEO-Sat j which occurs at the next LEO-Sats, i.e., LEO-Sats $j+2, \cdots, J$, or LEO-Sat $j+1$ suffers from the interfering signals transmitted by the behind LEO-Sats $j, \cdots, j-1$, meaning that (1) becomes

$$C_j = \log_2\left(\frac{P_{Leo,j} d_{j,j+1}^{-\alpha} G_{j,j+1}}{\sum_{i=0}^{j-1} P_{Leo,i} d_{i,j+1}^{-\alpha} G_{i,j+1} + \sigma^2}\right), \tag{38}$$

In Fig. 11, we demonstrate beamforming at LEO-Sats in multi-hop transmissions. It is observable that when the LEO-Sats are not aligned in a straight line, LEO-Sat j might experience reduced interference from LEO-Sats $0, \cdots, j-2$.

Therefore, for a Ω_j given in (20), the transmission rate from LEO-Sat j to LEO-Sat $j+1$ must satisfy the following condition :

$$\Omega_j \leq \Delta C_j, \quad j = 0, 1, \cdots, J. \tag{39}$$

where Δ is the local access network to backhaul bandwidth ratio. Given that the backhaul link is required to carry the aggregate traffic of all users, it is expected that $\Delta \geq 1$.

5.1.2 Downlink and Uplink Capacity of Local Access Networks

As shown in Fig. 8, it is expected that every LEO-Sat may provide a downward beam to support the users inside its Footprint.

- **Downlink within a footprint :** As mentioned in [57], assuming symmetrically that the channels from the LEO-Sat to the associated ground users have the same characteristics, the total rate of downlink of local access network j we can obtain from From (2) as,

$$D_{\mathrm{L},j} = \mathbb{E}\left[\log_2\left(1+\frac{P_{Loc,j}g^d_{j,k}}{\sigma^2}\right)\right], \tag{40}$$

  The LoS path dominates the air-to-ground channel, as described in [58]. As a result, we can characterize $g^d_{j,k}$ as:

$$g^d_{j,k} = \kappa d^{-\alpha}_{j,k}, \tag{41}$$

  where κ is constant. Since LEO-Sat are at high altitude $d_{j,k} \approx d_j$ for all k, $D_{\mathrm{L},j}$ can be approximated as

$$D_{\mathrm{L},j} \approx \log_2\left(1+\frac{P_{Loc,j}}{H_j}\right), \tag{42}$$

  where $H_j = \dfrac{\sigma^2}{\kappa} d^{\alpha}_j$. Assuming that a downlink transmission system with the maximum capacity is used, it can be shown that

$$\Upsilon_j = D_{\mathrm{L},j} \approx \log_2\left(1+\frac{P_{Loc,j}}{H_j}\right),\ j = 1,2,\cdots,J. \tag{43}$$

- **Uplink within a footprint :** From (3), we can the obtain uplink's total data transmission

rate as:

$$U_{\mathrm{L},j} = \mathbb{E}\left[\log_2\left(1+\frac{P_g\sum_{i=1}^{N_j} g_{j,i}^u}{\sigma^2}\right)\right], \tag{44}$$

Assuming that uplink transmissions use a capacity-achieving method, we have

$$\beta_j = U_{\mathrm{L},j},\ j = 1,2,\cdots,J. \tag{45}$$

As can be observed from (44), β_j is dependent on the number of ground users in the footprint, P_g's ground user transmit power, and the uplink channel coefficients, $g_{j,k}^u$. Hence, we assume that the β_j's are given.

5.2 Total Transmit Power Minimization Problem

An optimization problem can be formulated to allocate power among LEO-Sats, ensuring the support of given downlink and uplink transmission rates in local access networks. Specifically, when the values of Υ_j's and β_j's are provided, the problem of minimizing the total power can be formulated as follows:

$$\min_{P_0,\cdots,P_j} \sum_{j=0}^{J} P_j$$

subject to

$$\Omega_j = \sum_{i=j+1}^{J} \Upsilon_i + \sum_{i=1}^{j} \beta_i \ \leq\ \Delta C_j, \qquad j = 0,1,\cdots,J. \tag{46}$$

Since the values of Υ_j's are provided, we can infer that

$$P_j \geq P_{Loc,j} = H_j(2^{\Upsilon_j}-1). \tag{47}$$

Lemma: Let $P_j^*,\ j = 0,1,\cdots,J$, denote the solution of (46) and $P_{Leo,j}^* = P_j^* - P_{Loc,j},\ j = 0,1,\cdots,J$ (for LEO-Sat 0 or source gBs, we have $P_0 = P_{Leo,0}$). Here, $P_{Loc,j}$ is constant as the

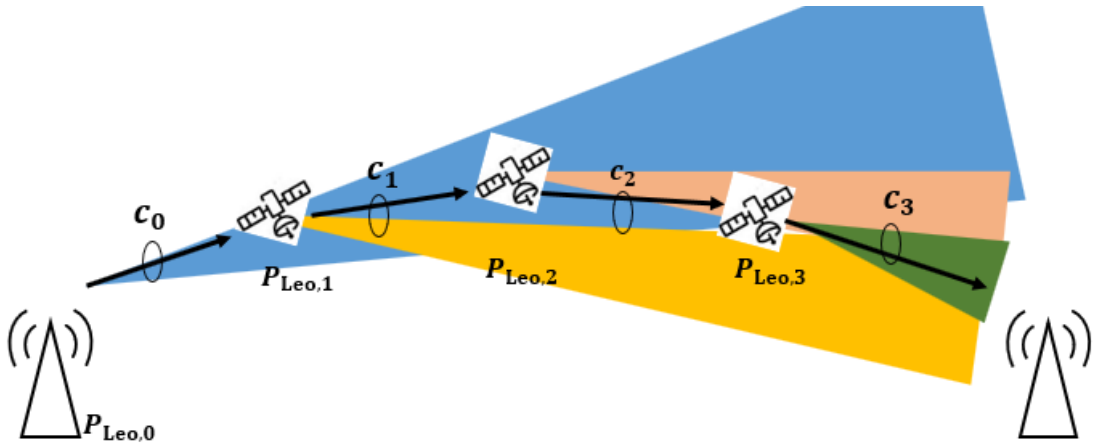

Fig. 11. Beams towards the next LEO-Sats in multi-hop transmissions.

Υ_j's are known as in (47). Consequently, $P^*_{Leo,j}$ can be recursively determined as follows:

$$P^*_{Leo,j} = (2^{\frac{\Omega_j}{\Delta}} - 1)\frac{\sum_{i=0}^{j-1} P^*_{Leo,i} d^{-\alpha}_{i,j+1} G_{i,j+1} + \sigma^2}{d^{-\alpha}_{i,j+1} G_{i,j+1}} \quad , j = 0, 1, \cdots, J. \tag{48}$$

Proof : Given the fixed value of $P_{Loc,m}$, minimizing the total transmit power is essentially equivalent to minimizing the $\sum_{j=0}^{J} P_{Leo,j}$ for $j = 0$, $P^*_{Leo,0} = P^*_0$ in (48) is the minimum transmit power of LEO-Sat 0 to meet the constraint in (46). For LEO-Sat 1, its transmit power LEO-link 1 is to satisfy

$$\frac{\Omega_1}{\Delta} \leq C_1 = \log_2\left(1 + \frac{P_{Leo,1} d^{-\alpha}_{1,2} G_{1,2}}{P_{Leo,0} d^{-\alpha}_{0,2} G_{0,2} + \sigma^2}\right), \tag{49}$$

In order to minimize $P_{Leo,1}$, we select the minimum value between $P_{Leo,0}$ and $P^*_{Leo,0}$. Consequently, the minimum value of $P_{Leo,1}$, while satisfying (49), can be obtained from (48). This process can be iterated for the subsequent LEOs, leading to the minimum $\sum_{j=0}^{J} P_{Leo,j}$ or the minimum of the total backhaul transmission power. This completes the proof.

Thus, by using (48), we can determine the optimal way to allocate LEO-Sat power so as to minimize the total transmit power of the LEO-Sats while maintaining the necessary data rates for ground users for both uplink and downlink transmissions .

Remarks :

- The transmit power may be substantial for a large value of J. To illustrate this, let's

examine a scenario with $J = 3$. Referring to the initial constraint in (46), we obtain the following:

$$\begin{aligned}
&\Upsilon_1 + \Upsilon_2 + \Upsilon_3 \leq \Delta C_0 \\
&\beta_1 + \Upsilon_2 + \Upsilon_3 \leq \Delta C_1 \\
&\beta_1 + \beta_2 + \Upsilon_3 \leq \Delta C_2 \\
&\beta_1 + \beta_2 + \beta_3 \leq \Delta C_3.
\end{aligned} \tag{50}$$

Considering that the β_j's are known from (38), the last inequality shows

$$P_{Leo,3} \geq \left(2^{\frac{\beta_1+\beta_2+\beta_3}{\Delta}} - 1\right) \times \frac{P^*_{Leo,0} d^{-\alpha}_{0,3} G_{0,3} + P^*_{Leo,1} d^{-\alpha}_{1,3} G_{1,3} + P^*_{Leo,2} d^{-\alpha}_{2,3} G_{2,3} + \sigma^2}{d^{-\alpha}_{3,4} G_{3,4}}. \tag{51}$$

Therefore, for a given set of LEO-Sats, the backhaul transmission power of LEO-Sat 3 to the sink gNB, $P_{Leo,3}$, depends on $P_{Leo,j}$, $j = 0, 1, \cdots, 2$. Furthermore, $P_{Leo,2}$ is a function of $P_{Leo,j}$, $j = 0, \cdots, 1$, and $P_{Leo,j}$ generally increases as j does. As a result, as J increases, the total backhaul transmission power does too. Due to limited transmit power of LEO-Sats, minimal J is required.

- Because the transmission power of LEO-Sats cannot be set arbitrarily high, the capacity of LEO-link n becomes constrained. Therefore, in order to meet the inequalities in (50), Δ must grow as J increases. This suggests that since the LEO-link's bandwidth is limited, a lower J is preferable.

5.3 Simulation Result

We assume that for each local access network

$$\Upsilon_j = \log_2\left(1+\frac{P_{Loc}d_j^{-\alpha}}{\sigma^2}\right)$$
$$\beta_j = \log_2\left(1+\frac{P_g N_j d_j^{-\alpha}}{\sigma^2}\right),\ j=1,2,\cdots,J. \tag{52}$$

where N_j is the average number of users in each footprint.balanced. It is further assumed that the uplink and downlink rates within local access networks are

$$\text{SNR}_{\text{loc,up}} = \frac{P_g N_j d_j^{-\alpha}}{\sigma^2} \quad \text{and} \quad \text{SNR}_{\text{loc,dw}} = \frac{P_{Loc}d_j^{-\alpha}}{\sigma^2}, \tag{53}$$

which are known as the local SNR for uplink and downlink respectively.

The following parameters are fixed in the simulations:

σ^2 =-174 dBm/Hz, $\alpha = 2$, and $G_{i,j} = 40$ dB.

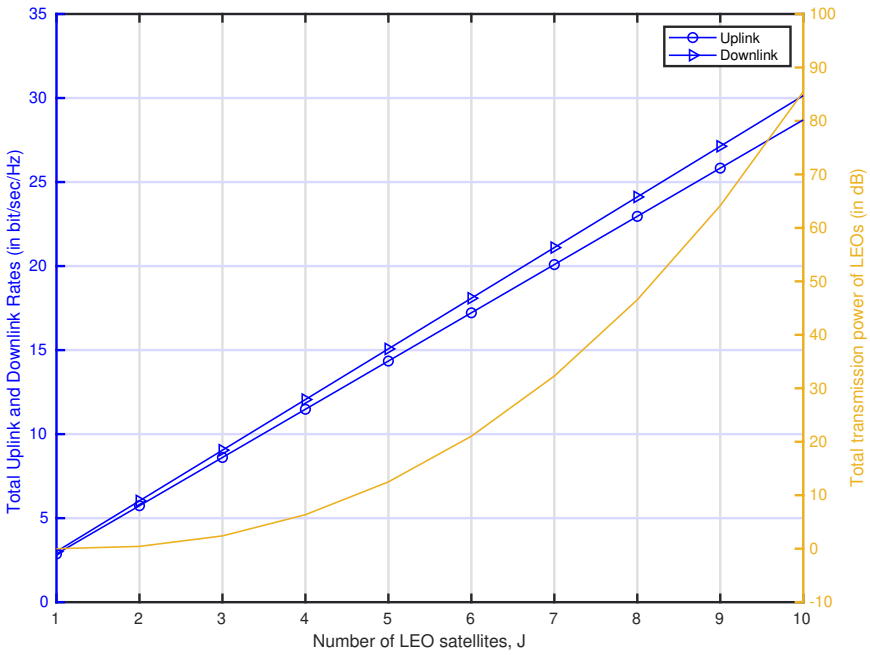

Fig. 12. LEO-Sat network performance for different numbers of LEO-Sats J, when $\text{SNR}_{\text{loc,up}} = 8.5$ dB, $\text{SNR}_{\text{loc,dw}} = 8$ dB and $\Delta = 4$.

In Fig. 12, the performance of LEO-Sat networks is presented for different numbers of LEO-

Sats, J, when $\text{SNR}_{\text{loc}} = 8$ dB. Although J varies, it is assumed that $\Delta = 4$. However, $\Delta = J$ in Fig. 13, since Υ and β represent the total transmission rates, they increase with J in both scenarios. Nevertheless, there is a difference in the increase of the overall backhaul transmission power of LEO-Sats, (i.e $\sum_{j=0}^{J} P_{Leo,j}$)

When Δ is fixed, the total backhaul transmission power increases quickly when $J > \Delta$, as seen in Fig. 12. In contrast, when $\Delta = J$ (as in Fig. 13), the total backhaul transmission power increases slowly . Therefore, given that the means of Υ_j and β_j are independent of the number of J, it is required to increase the bandwidth of backhaul networks with J (by linearly increasing Δ), except a high transmission power is available to raise the backhaul link capacity, C_j,

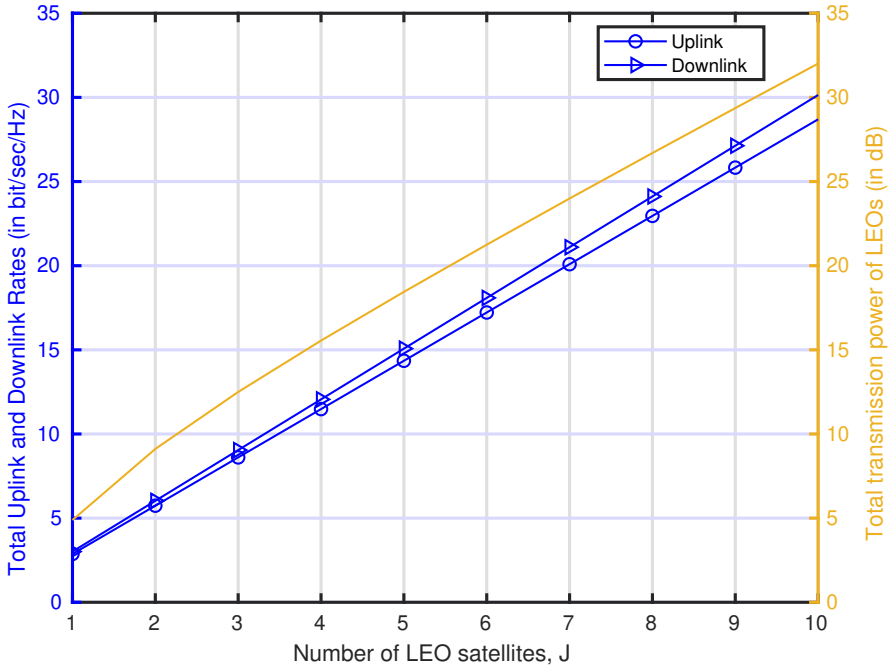

Fig. 13. LEO-Sat network performance for different numbers of LEO-Sats J, when $\text{SNR}_{\text{loc,up}} = 8.5$ dB, $\text{SNR}_{\text{loc,dw}} = 8$ dB and $\Delta = J$.

Chapter 6 – Conclusion

Integrated access and backhaul (IAB) represents a significant advancement in 5G New Radio (NR), facilitating swift and economical deployment of millimeter-wave (mmWave) technology by enabling self-backhauling within the same spectrum. Such deployments offer remarkable coverage at cell edges, while substantially diminishing the need for fiber infrastructure. Non-terrestrial Networks have been officially introduced in fifth-generation access networks since Rel-17 where the Satellite Access Node has been defined. Of this Non-terrestrial Networks LEO satellites stand out because they offer rapid, low-latency connectivity, which is crucial for time-sensitive applications like remote surgery or autonomous vehicles where even slight delays could have significant repercussions. Positioned in a high altitude from the Earth's surface, LEO satellites can achieve remarkably low latency levels, making them comparable to terrestrial networks in terms of responsiveness. Therefore, in our study, we implemented a multi-LEO-satellite network model for IAB, to cater to ground users who lack direct connectivity to gNBs. We evaluated the network's performance based on packet transmission delay and its reliability, as indicated by outage probability metrics. LEO-Sats can be seen as relay nodes that help connect ground users to gNBs.

This thesis has accomplished three main objectives: A wireless multi-hop transmission model of LEO-Sat-networks is proposed for integrated access and backhaul (IAB) to support ground users unable to directly communicate with gNBs. The traffic flows for uplink and downlink transmissions are characterized using the channel capacity of local access and backhaul links. The performance of the proposed multi-LEO-Satellites model for integrated access and backhaul is evaluated with a focus on latency. This assessment includes analyzing the packet transmission delay within the LEO-Satellite-based backhaul network and access network. Additionally, analytical expressions for outage probabilities are derived for both the backhaul link, comprising inter-LEO satellite communication, and access networks linking LEO satellites with ground users. Finally, an optimization problem is formulated to minimize the total transmit power of LEO-Sats for a given path, subject to the data rates of uplink and downlink transmissions of ground users along the path. The solution obtained from this optimization problem is then utilized for the power allocation of LEO-Sats.

Future work

Further research into Multi-LEO Satellite Networks for IAB may concentrate on reducing the effects of Doppler effects on communication links through the development of innovative signal processing methods and adaptive algorithms that can adjust for frequency shifts brought about by satellite motion, thereby enhancing link reliability. Further enhancing network efficiency, adaptability, and fault tolerance is the use of machine learning techniques for network optimization, such as anomaly detection, predictive analytics, and adaptive resource allocation based on real-time conditions. In addition, network performance can be maximized, latency can be reduced, and overall user experience can be improved in Multi-LEO satellite environments by using machine learning for dynamic resource allocation, such as bandwidth, power, and routing paths. In the analysis of throughput and optimal power allocation, the optimization of LEO-Sats' locations is not included. However, optimizing the locations of LEO-Sats, along with ground users, has the potential to reduce backhaul transmission power. This aspect could be could be investigated in future studies.

References

1. H. Willebrand and B. Ghuman, "Fiber optics without fiber," *IEEE Spectrum*, vol. 38, no. 8, pp. 40–45, 2001.
2. O. Teyeb, A. Muhammad, G. Mildh, E. Dahlman, F. Barac, and B. Makki, "Integrated access backhauled networks," in *2019 IEEE 90th Vehicular Technology Conference (VTC2019-Fall)*, 2019, pp. 1–5.
3. J. Peisa, P. Persson, S. Parkvall, E. Dahlman, A. Grøvlen, C. Hoymann, and D. Gerstenberger, "5G evolution: 3gpp releases 16 17 overview," *Ericsson Technology Review*, vol. 2020, no. 2, pp. 2–13, 2020.
4. M. Polese, M. Giordani, T. Zugno, A. Roy, S. Goyal, D. Castor, and M. Zorzi, "Integrated access and backhaul in 5G mmwave networks: Potential and challenges," *IEEE Communications Magazine*, vol. 58, no. 3, pp. 62–68, 2020.
5. M. Cudak, A. Ghosh, A. Ghosh, and J. Andrews, "Integrated access and backhaul: A key enabler for 5G millimeter-wave deployments," *IEEE Communications Magazine*, vol. 59, no. 4, pp. 88–94, 2021.
6. Y. Sadovaya, D. Moltchanov, W. Mao, O. Orhan, S.-p. Yeh, H. Nikopour, S. Talwar, and S. Andreev, "Integrated access and backhaul in millimeter-wave cellular: Benefits and challenges," *IEEE Communications Magazine*, vol. 60, no. 9, pp. 81–86, 2022.
7. 3rd Generation Partnership Project, "Study on integrated access and backhaul," 3rd Generation Partnership Project, Tech. Rep. TR 38.874, December 2018, release 15. [Online]. Available: https://www.3gpp.org/dynareport/38874.htm
8. ——, "Nr and ng-ran overall description (stage 2)," 3rd Generation Partnership Project, Tech. Rep. V17.3.0, December 2022, release 17. [Online]. Available: https://www.3gpp.org/dynareport/38300.htm
9. W. Chen, X. Lin, J. Lee, A. Toskala, S. Sun, C. F. Chiasserini, and L. Liu, "5G-advanced toward 6G: Past, present, and future," *IEEE Journal on Selected Areas in Communications*, vol. 41, no. 6, pp. 1592–1619, 2023.
10. D. Soldani and A. Manzalini, "Horizon 2020 and beyond: On the 5G operating system for a true digital society," *IEEE Vehicular Technology Magazine*, vol. 10, no. 1, pp. 32–42, 2015.
11. I. Union, "Imt traffic estimates for the years 2020 to 2030," *Report ITU*, vol. 2370, 2015.

12. N. Bhushan, J. Li, D. Malladi, R. Gilmore, D. Brenner, A. Damnjanovic, R. T. Sukhavasi, C. Patel, and S. Geirhofer, "Network densification: the dominant theme for wireless evolution into 5G," *IEEE Communications Magazine*, vol. 52, no. 2, pp. 82–89, 2014.
13. M. Agiwal, A. Roy, and N. Saxena, "Next generation 5g wireless networks: A comprehensive survey," *IEEE communications surveys & tutorials*, vol. 18, no. 3, pp. 1617–1655, 2016.
14. H. A. Willebrand and B. S. Ghuman, "Fiber optics without fiber," *IEEE spectrum*, vol. 38, no. 8, pp. 40–45, 2001.
15. C. B. Czegledi, M. Hörberg, M. Sjödin, P. Ligander, J. Hansryd, J. Sandberg, J. Gustavsson, D. Sjöberg, D. Polydorou, and D. Siomos, "Demonstrating 139 gbps and 55.6 bps/hz spectrum efficiency using 8× 8 mimo over a 1.5-km link at 73.5 ghz," in *2020 IEEE/MTT-S International Microwave Symposium (IMS)*. IEEE, 2020, pp. 539–542.
16. S. Dang, O. Amin, B. Shihada, and M.-S. Alouini, "What should 6G be?" *Nature Electronics*, vol. 3, no. 1, pp. 20–29, 2020.
17. A. Hoglund, X. Lin, O. Liberg, A. Behravan, E. A. Yavuz, M. Van Der Zee, Y. Sui, T. Tirronen, A. Ratilainen, and D. Eriksson, "Overview of 3gpp release 14 enhanced NB-IoT," *IEEE network*, vol. 31, no. 6, pp. 16–22, 2017.
18. S. Rangan, T. S. Rappaport, and E. Erkip, "Millimeter-wave cellular wireless networks: Potentials and challenges," *Proceedings of the IEEE*, vol. 102, no. 3, pp. 366–385, 2014.
19. S. Parkvall, E. Dahlman, A. Furuskar, and M. Frenne, "Nr: The new 5G radio access technology," *IEEE Communications Standards Magazine*, vol. 1, no. 4, pp. 24–30, 2017.
20. X. Lin, J. Li, R. Baldemair, J.-F. T. Cheng, S. Parkvall, D. C. Larsson, H. Koorapaty, M. Frenne, S. Falahati, A. Grovlen *et al.*, "5g new radio: Unveiling the essentials of the next generation wireless access technology," *IEEE Communications Standards Magazine*, vol. 3, no. 3, pp. 30–37, 2019.
21. C. Dehos, J. L. González, A. De Domenico, D. Ktenas, and L. Dussopt, "Millimeter-wave access and backhauling: The solution to the exponential data traffic increase in 5G mobile communications systems?" *IEEE communications magazine*, vol. 52, no. 9, pp. 88–95, 2014.
22. C. Madapatha, B. Makki, C. Fang, O. Teyeb, E. Dahlman, M.-S. Alouini, and T. Svensson, "On integrated access and backhaul networks: Current status and potentials," *IEEE Open Journal of the Communications Society*, vol. 1, pp. 1374–1389, 2020.
23. A. 3GPP, "Ng-ran; architecture description," 2020.

24. E. Yaacoub and M.-S. Alouini, "A key 6G challenge and opportunity—connecting the base of the pyramid: A survey on rural connectivity," *Proceedings of the IEEE*, vol. 108, no. 4, pp. 533–582, 2020.

25. M. Kishk, A. Bader, and M.-S. Alouini, "Aerial base station deployment in 6G cellular networks using tethered drones: The mobility and endurance tradeoff," *IEEE Vehicular Technology Magazine*, vol. 15, no. 4, pp. 103–111, 2020.

26. A. Perez, A. Fouda, and A. S. Ibrahim, "Ray tracing analysis for UAV-assisted integrated access and backhaul millimeter wave networks," in *2019 IEEE 20th International Symposium on" A World of Wireless, Mobile and Multimedia Networks"(WoWMoM)*. IEEE, 2019, pp. 1–5.

27. Y. Hu, M. Chen, and W. Saad, "Joint access and backhaul resource management in satellite-drone networks: A competitive market approach," *IEEE Transactions on Wireless Communications*, vol. 19, no. 6, pp. 3908–3923, 2020.

28. M. Mozaffari, W. Saad, M. Bennis, and M. Debbah, "Unmanned aerial vehicle with underlaid device-to-device communications: Performance and tradeoffs," *IEEE Transactions on Wireless Communications*, vol. 15, no. 6, pp. 3949–3963, 2016.

29. Z. Wang, R. Liu, Q. Liu, J. S. Thompson, and M. Kadoch, "Energy-efficient data collection and device positioning in UAV-assisted IoT," *IEEE Internet of Things Journal*, vol. 7, no. 2, pp. 1122–1139, 2020.

30. D.-H. Tran, V.-D. Nguyen, S. Chatzinotas, T. X. Vu, and B. Ottersten, "UAV relay-assisted emergency communications in IoT networks: Resource allocation and trajectory optimization," *IEEE Transactions on Wireless Communications*, vol. 21, no. 3, pp. 1621–1637, 2022.

31. I. Valiulahi and C. Masouros, "Multi-UAV deployment for throughput maximization in the presence of co-channel interference," *IEEE Internet of Things Journal*, vol. 8, no. 5, pp. 3605–3618, 2021.

32. L. Zhang and N. Ansari, "On the number and 3-d placement of in-band full-duplex enabled drone-mounted base-stations," *IEEE Wireless Communications Letters*, vol. 8, no. 1, pp. 221–224, 2018.

33. E. Kalantari, M. Z. Shakir, H. Yanikomeroglu, and A. Yongacoglu, "Backhaul-aware robust 3D drone placement in 5G+ wireless networks," in *2017 IEEE international conference on communications workshops (ICC workshops)*. IEEE, 2017, pp. 109–114.

34. C. T. Cicek, H. Gultekin, B. Tavli, and H. Yanikomeroglu, "Backhaul-aware optimization of UAV base station location and bandwidth allocation for profit maximization," *IEEE Access*, vol. 8, pp.

154 573–154 588, 2020.

35. M. Gapeyenko, V. Petrov, D. Moltchanov, S. Andreev, N. Himayat, and Y. Koucheryavy, "Flexible and reliable UAV-assisted backhaul operation in 5G mmwave cellular networks," *IEEE Journal on Selected Areas in Communications*, vol. 36, no. 11, pp. 2486–2496, 2018.
36. Z. Lin, M. Lin, B. Champagne, W.-P. Zhu, and N. Al-Dhahir, "Secure beamforming for cognitive satellite terrestrial networks with unknown eavesdroppers," *IEEE Systems Journal*, vol. 15, no. 2, pp. 2186–2189, 2021.
37. L. Zhen, T. Sun, G. Lu, K. Yu, and R. Ding, "Preamble design and detection for 5G enabled satellite random access," *IEEE Access*, vol. 8, pp. 49 873–49 884, 2020.
38. Z. Lin, M. Lin, T. de Cola, J.-B. Wang, W.-P. Zhu, and J. Cheng, "Supporting IoT with rate-splitting multiple access in satellite and aerial-integrated networks," *IEEE Internet of Things Journal*, vol. 8, no. 14, pp. 11 123–11 134, 2021.
39. M. Shaat, E. Lagunas, A. I. Perez-Neira, and S. Chatzinotas, "Integrated terrestrial-satellite wireless backhauling: Resource management and benefits for 5G," *IEEE Vehicular Technology Magazine*, vol. 13, no. 3, pp. 39–47, 2018.
40. B. Di, H. Zhang, L. Song, Y. Li, and G. Y. Li, "Data offloading in ultra-dense LEO-based integrated terrestrial-satellite networks," in *2018 IEEE Global Communications Conference (GLOBECOM)*, 2018, pp. 1–6.
41. R. Deng, B. Di, S. Chen, S. Sun, and L. Song, "Ultra-dense LEO satellite offloading for terrestrial networks: How much to pay the satellite operator?" *IEEE Transactions on Wireless Communications*, vol. 19, no. 10, pp. 6240–6254, 2020.
42. Z. Abdullah, S. Kisseleff, E. Lagunas, V. N. Ha, F. Zeppenfeldt, and S. Chatzinotas, "Integrated access and backhaul via satellites," in *2023 IEEE 34th Annual International Symposium on Personal, Indoor and Mobile Radio Communications (PIMRC)*, 2023, pp. 1–6.
43. E. Lagunas, S. Maleki, L. Lei, C. Tsinos, S. Chatzinotas, and B. Ottersten, "Carrier allocation for hybrid satellite-terrestrial backhaul networks," in *2017 IEEE International Conference on Communications Workshops (ICC Workshops)*. IEEE, 2017, pp. 718–723.
44. B. Di, H. Zhang, L. Song, Y. Li, and G. Y. Li, "Data offloading in ultra-dense LEO-based integrated terrestrial-satellite networks," in *2018 IEEE Global Communications Conference (GLOBECOM)*. IEEE, 2018, pp. 1–6.
45. R. Deng, B. Di, S. Chen, S. Sun, and L. Song, "Ultra-dense leo satellite offloading for terrestrial

networks: How much to pay the satellite operator?" *IEEE Transactions on Wireless Communications*, vol. 19, no. 10, pp. 6240–6254, 2020.

46. M. Handley, "Using ground relays for low-latency wide-area routing in megaconstellations," in *Proceedings of the 18th ACM Workshop on Hot Topics in Networks*, 2019, pp. 125–132.
47. G. Pan, J. Ye, J. An, and S. Alouini, "Latency versus reliability in LEO mega-constellations: Terrestrial, aerial, or space relay," *IEEE Transactions on Mobile Computing*, 2022.
48. J. Shi, J. Hu, Y. Yue, X. Xue, W. Liang, and Z. Li, "Outage probability for otfs based downlink leo satellite communication," *IEEE Transactions on Vehicular Technology*, vol. 71, no. 3, pp. 3355–3360, 2022.
49. G. Pan, J. Ye, J. An, and M.-S. Alouini, "Latency versus reliability in LEO mega-constellations: Terrestrial, aerial, or space relay?" *IEEE Transactions on Mobile Computing*, vol. 22, no. 9, pp. 5330–5345, 2023.
50. P. Viswanath and D. Tse, "Fundamentals of wireless communication," 2005.
51. T. Darwish, G. K. Kurt, H. Yanikomeroglu, M. Bellemare, and G. Lamontagne, "LEO satellites in 5G and beyond networks: A review from a standardization perspective," *IEEE Access*, vol. 10, pp. 35 040–35 060, 2022.
52. B. Di, H. Zhang, L. Song, Y. Li, and G. Y. Li, "Ultra-dense LEO: Integrating terrestrial-satellite networks into 5G and beyond for data offloading," *IEEE Transactions on Wireless Communications*, vol. 18, no. 1, pp. 47–62, 2019.
53. A. Sabharwal, P. Schniter, D. Guo, D. W. Bliss, S. Rangarajan, and R. Wichman, "In-band full-duplex wireless: Challenges and opportunities," *IEEE Journal on Selected Areas in Communications*, vol. 32, no. 9, pp. 1637–1652, 2014.
54. B. Maham, "Performance analysis of ultra-dense millimeter wave cloud-RAN under blockage and interference," in *2021 IEEE Global Communications Conference (GLOBECOM)*, 2021, pp. 1–6.
55. M. K. Simon and M.-S. Alouini, *Digital communication over fading channels*. New York: Wiley, 2001.
56. A. Ospanova, B. Maham, and R. C. Kizilirmak, "Delay-outage analysis of multi-LEO satellites communication system," *IEEE Access*, vol. 11, pp. 124 509–124 523, 2023.
57. D. Tse and P. Viswanath, *Fundamentals of Wireless Communication*. Cambridge University Press, 2005.
58. A. Al-Hourani, S. Kandeepan, and S. Lardner, "Optimal lap altitude for maximum coverage,"

IEEE Wireless Communications Letters, vol. 3, no. 6, pp. 569–572, 2014.